

Manufacturing of Poly(vinylidene fluoride) and Evaluation of its Mechanical Properties

Daniel M. Esterly

Virginia Polytechnic Institute and State University

Masters of Science
in
Materials Science and Engineering

Dr. Brian J. Love
Dr. Donald Leo
Dr. Daniel Inman

August 9, 2002
Blacksburg, Virginia

Piezoelectric Polymers, Cryogenic Milling of Polymers, PVDF, In-Situ Mechanical Testing of
Electrically Biased Films

Copyright 2002, Daniel M. Esterly



Manufacturing of Poly(vinylidene fluoride) and Evaluation of its Mechanical Properties

Daniel M. Esterly

Abstract

Poly(vinylidene fluoride) (PVDF) receives an increasing amount of attention because it exhibits the strongest piezoelectric response of any commercially available polymer. These piezoelectric properties have proved useful as actuators and sensors. Current manufacturing processes limit PVDF to thin films and restricting their uses largely to sensors. Further applications utilizing the changes in mechanical properties of piezoelectric polymers are being realized. Evaluating to what extent the mechanical properties will change with applied electric field and finding new ways to manufacture PVDF will lead to new applications of piezoelectric polymers.

In-situ mechanical testing of biased piezoelectric PVDF films successfully measured changes in loss and storage modulus. In-situ creep testing measured an increase in stiffness while in-situ dynamic mechanical analysis (DMA) measured an overall decrease in loss and storage modulus. Differences in results between the two experiments are attributed to orientation of the polymer and piezoelectric forces acting on the equipment. DMA results are accepted as being the most accurate and measured changes of over 20% in elastic modulus. Results were believed to be greatly influenced by attached electrodes and actuation forces.

Cryogenic mechanical milling successfully converted α phase PVDF powder to β phase as measured with wide-angle x-ray diffraction. This is the first recorded instance of β phase powders forming from the α phase through ball milling. These β phase powders maintained their crystal structure during compression molding at 70°C.



Table of Contents

Chapter 1	<u>Introduction and Background</u>	1
1.1	<u>Introduction and Motivation</u>	1
1.2	<u>Piezoelectrics</u>	1
1.3	<u>Polymer Piezoelectrics Background and History</u>	3
1.4	<u>Applications of Piezoelectric Polymers</u>	4
1.5	<u>Properties of Poly(vinylidene fluoride), PVDF</u>	5
1.6	<u>Stable Polymorphism of PVDF</u>	7
1.7	<u>Poling of PVDF</u>	11
1.8	<u>Phase Transformations</u>	13
1.9	<u>Milling</u>	14
Chapter 2	<u>Experimental Equipment and Procedures</u>	16
2.1	<u>Sample Preparation</u>	16
2.1.1	<u>Hot Pressing films</u>	16
2.1.2	<u>Mechanical Ball Millings</u>	17
2.1.3	<u>Preparation of Purchased films</u>	18
2.1.4	<u>Annealing β Phase PVDF Films</u>	19
2.2	<u>Material Characterization</u>	19
2.2.1	<u>Wide Angle X-ray Diffraction (WAX)</u>	20
2.2.2	<u>Scanning Electron Microscopy (SEM)</u>	20
2.3	<u>In-Situ Mechanical Testing</u>	20
2.3.1	<u>In-Situ Creep Testing</u>	21
2.3.2	<u>In Situ Dynamic Mechanical Analysis (DMA)</u>	23
Chapter 3	<u>Results and Discussion</u>	27
3.1	<u>Sample Preparation</u>	27
3.1.1	<u>Hot Pressing Films</u>	27
3.1.2	<u>Preparation of Purchased films</u>	27
3.2	<u>Material Characterization</u>	28
3.2.1	<u>Wide Angle X-ray Diffraction (WAX)</u>	28
3.2.2	<u>Scanning Electron Microscopy (SEM)</u>	34
3.3	<u>In-Situ Mechanical Testing</u>	38
3.3.1	<u>In-Situ Creep Testing</u>	39
3.3.2	<u>In Situ (DMA)</u>	43
Chapter 4	<u>Conclusions</u>	51
4.1	<u>Sample Preparation</u>	51
4.1.1	<u>Hot Pressing Films</u>	51
4.1.2	<u>Preparation of Purchased Films</u>	51
4.2	<u>Material Characterization</u>	51
4.3	<u>In-Situ Mechanical Testing</u>	52
4.3.1	<u>Creep Testing</u>	52
4.3.2	<u>In-Situ Dynamic Mechanical Analysis</u>	53
4.4	<u>Recommendations for Future Work</u>	54
Bibliography		56
Appendix		59

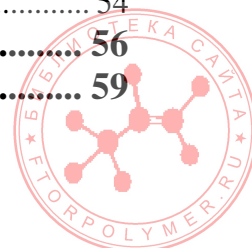


Table of Figures

Figure 1.1 Structure of α PVDF (left) and β PVDF (right)	7
Figure 1.2 Diagram of van der Waals forces between the atoms in PVDF.	8
Figure 1.3 Unit cell structure of α phase PVDF.	10
Figure 1.4 Crystalline structure of β phase poly(vinylidene fluoride).	11
Figure 1.5 Example of the alignment of dipoles within β phase PVDF.	12
Figure 1.6 Obtaining each of the crystalline phases of PVDF	13
Figure 2.1 Diagram of shaker ball mill used during mechanical milling	18
Figure 2.2 In-situ creep diagram.	21
Figure 2.3 In-situ creep experiment with the Texture Analyzer.	22
Figure 2.4 Diagram of three point bend setup used in the Perkin Elmer DMA.	24
Figure 2.5 PVDF film in three point bend with electrodes attached.	24
Figure 2.6 Dimensions of samples used in extension in the DMA.	25
Figure 2.7 PVDF sample in extension with electrodes attached.	26
Figure 3.1 X-ray analysis of annealed purchased PVDF samples.	29
Figure 3.2 X-ray analysis of hot pressed films	31
Figure 3.3 X-ray comparison of purchased and drawn films.	32
Figure 3.4 X-ray comparison of drawn and undrawn films.	32
Figure 3.5 X-ray data of milled Kynar® powder	33
Figure 3.6 X-ray data of milled Kynar® powder	34
Figure 3.7 SEM Pictures of milled and unmilled Kynar® powder.	36
Figure 3.8 Comparison of particle sizes between milled and unmilled Kynar® powder	37
Figure 3.9 SEM pictures of sintered PVDF films.	38
Figure 3.10 In-situ creep testing of biased PVDF film	39
Figure 3.11 In-situ creep testing of biased PVDF film	40
Figure 3.12 Representation of the model use to measure the creep of PVDF films.	41
Figure 3.13 Representative curve fitting of recorded data to the four-element model.	42
Figure 3.14 Results of the annealed films under in-situ loading.	43
Figure 3.15 In situ biased PVDF films under DMA in three point bend	46
Figure 3.16 In situ biased PVDF films under DMA in three point bend	47
Figure 3.17 In situ biased PVDF films under DMA in extension	48
Figure 3.18 In situ biased PVDF films under DMA in extension	49
Figure A.1 X-Ray diffraction of unmilled, compression molded PVDF powder	59
Figure A.2 X-Ray diffraction of milled, compression molded PVDF powder	59
Figure A.3 X-Ray diffraction of PVDF films annealed in an oven and hot press	60
Figure A.4 In-Situ creep test of biased PVDF film	60
Figure A.5 In-Situ creep test of biased, annealed PVDF film.	61
Figure A.6 DMA of biased PVDF in three point bend	61
Figure A.7 DMA of biased PVDF in three point bend	62
Figure A.8 DMA of biased PVDF in extension	62
Figure A.9 DMA of biased PVDF in extension	63
Figure A.10 DMA of biased PVDF in extension	63
Figure A.11 DMA of biased PVDF in extension	64
Figure A.12 DMA of biased PVDF in extension	64

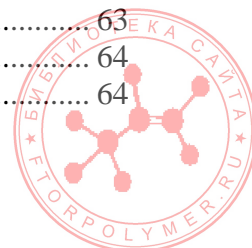


Figure A.13 DMA of biased PVDF in extension	65
Figure A.14 DSC of Poly(vinylidene fluoride)	65

Table of Tables

Table 1.1 Comparison of smart materials	3
Table 1.2 Piezoelectric coefficients of poly(vinylidene fluoride)	4
Table 1.3 Piezoelectric constants for some well know materials	4
Table 1.4 Dimensions of the unit cells for the crystalline structures of PVDF. (7,10)	10
Table 2.1 Temperature and pressure combinations of pressed PVDF films	17
Table 3.1 Crystal planes of PVDF's crystal phases	28
Table 3.2 Viscoelastic coefficients obtained from creep data	41
Table 3.3 Changes in storage modulus with applied voltage	44
Table 3.4 Changes in loss modulus with applied voltage	45
Table 3.5 Changes in Young's modulus with applied electric potential	45
Table 3.6 Changes in the frequency of observed peaks during DMA testing	50

Table of Equations

Equation 1.1 Stress strain relationship of piezoelectricity	2
Equation 3.1 Four element model of viscoelasticity	41
Equation 3.2 Relationship between Young's modulus and storage and loss moduli	45



Chapter 1 Introduction and Background

1.1 Introduction and Motivation

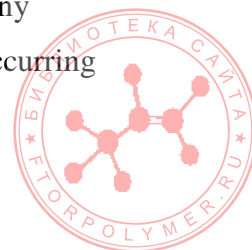
The β phase of poly(vinylidene fluoride) is, to date, the most responsive piezoelectric polymer. PVDF's strong piezoelectric response and chemical and mechanical durability make it a valuable material for use as sensors and actuators. However, the process used to manufacture PVDF's piezoelectric β phase is limited to drawn films. These films make ideal sensors because of their flexibility but limit PVDF's use as an actuator. Finding new ways to manufacture piezoelectric PVDF, including formation and processing of the β phase, can expand its use for actuation as well as sensing.

In addition to actuation and sensing the viscoelastic properties of piezoelectric polymers could also prove useful. By changing the viscoelastic properties such as storage and loss modulus as well as overall stiffness, PVDF could be used to actively resist deformation or isolate vibration. These properties can be evaluated with applied voltage using in-situ mechanical testing techniques.

1.2 Piezoelectrics

Piezoelectrics are a class of materials that can transfer mechanical energy to electrical energy and vice versa. The piezoelectric effect consists of a linear coupling between an applied electric field and an induced strain. In other words, an input of mechanical energy will produce an electrical polarization. The reverse phenomenon also occurs; applying an electrical polarization will cause changes in dimensions. The response of the material is proportional to the electric field or change in dimension. This predictable material property is extremely valuable in sensing and actuation ^(1, 2, 3, 4, 5).

Pierre and Jacques Curie discovered the piezoelectric effect in the late 1800's when they realized that certain materials deform when an electric potential is placed across them. The importance of such materials was quickly realized and it was soon found that quartz crystals could vibrate at various frequencies by applying electromagnetic radiation. By World War II, the U.S. Army used quartz crystals to send messages over radio waves. Since then, many different materials have been investigated for their piezoelectric response. Naturally occurring



crystals and other materials such as quartz, bone and wood were among the first to be evaluated. Synthetic materials are perhaps the most well known because they exhibit the largest measurable responses to electric fields. Ceramics like barium-titanate (BaTiO_3) and lead-zirconate-titanate (PZT) are some of the most popular materials currently used in industry ^(5, 6).

Piezoelectrics are part of a class of materials called ferroelectrics. Ferroelectric materials are substances that have an electric polarization reversible by an electric field. All piezoelectrics materials are ferroelectric in that they are naturally polarized or polarizable when exposed to specific conditions. However, not all ferroelectrics exhibit the same ability to produce an electric potential when deformed as do piezoelectrics. Ferroelectrics may also exhibit pyroelectric behavior, where a net change in potential occurs with changes in temperature ^(2, 7).

The response found in piezoelectrics occurs in few materials and depends greatly on the material's molecular arrangement. Piezoelectricity is a third-rank tensor property that is found only in acentric materials. Most of these materials are crystalline and their molecular structure allows the individual crystals within the material to act collectively producing a measurable net response. When these crystals are not oriented, there is no net response. Almost all materials are electrostrictive, in that they expand or contract in the presence of an electric field. The response of electrostrictive materials is very small and acts in all directions. Piezoelectrics only respond in one or two directions due to their asymmetric nature, and the response is useful in actuator and sensor applications. The small electrostrictive material response is not as useful as the piezoelectric response but stronger electrostrictive responses can influence material properties ^(2, 8).

Since the piezoelectric effect is a tensor quantity, a matrix provides a convenient expression to describe the behavior of the material in each direction. The defining equation for piezoelectric materials follows: ⁽⁹⁾

$$\{S\} = [s]\{T\} + [d]^T\{E\} \quad (1.1)$$

where:

$\{S\}$ = strain matrix

$\{T\}$ = stress matrix

$\{E\}$ = electric field matrix

$[s]$ = compliance matrix at constant electric field

$[d]^T$ = transpose piezoelectric strain matrix at constant stress



1.3 Polymer Piezoelectrics Background and History

Polymers are researched extensively as piezoelectrics because of their unique properties and advantages over other piezoelectrics. The piezoelectric response of polymers is less pronounced than those of single crystal inorganics, but polymers do have their advantages. Poly(vinylidene fluoride), in particular, has high chemical resistance, and high efficiency in converting mechanical energy to electrical. Polymers are easier to manufacture, often at lower temperatures, and can be formed more easily into custom shapes for use in complex operations. In addition, polymers are inherently flexible, have relatively low modulus and low mechanical impedance, with high sensitivity to mechanical loads. These properties make them more versatile than other piezoelectric materials for sensing and actuation. There are a few other semi-crystalline organic materials that show piezoelectric properties, but none have shown as same magnitude of response of poly(vinylidene fluoride) and its copolymers ^(1, 5, 7, 10, 11, 12).

Dr. Heiji Kawai discovered the piezoelectric properties of PVDF, in 1969. Furakawa and Johnson confirmed PVDF's piezoelectric nature in 1981 and identified the Curie point of 103°C. (The Curie point is the temperature above, which the piezoelectric effect breaks down.) Before 1969 the only materials that received much attention for their ferroelectric or piezoelectric properties were naturally occurring crystals, such as quartz, and man-made ceramics, such as barium titanate and lead zirconate titanate (PZT) ^(1, 3, 5, 7, 10, 13).

The benefits of using piezoelectric polymers can be seen in Table 1.1. Piezoelectric polymers are much more sensitive in responding to deformations and electric fields than ceramics and are much more durable ⁽¹⁴⁾.

Property	Piezoelectric Polymers	Piezo Ceramics	Shape Memory Alloys
Actuation Strain	2-5%	0.1-0.3%	<8%
Actuation Force (MPa)	0.1-3	30-40	about 700
Reaction Speed	μsec to sec	μsec to sec	sec to min
Density	1-2.5 g/cc	6-8 g/cc	5-6 g/cc
Driving Voltage	2 - 400V/μm	50-800V	NA
Power Consumption	m-Watts	Watts	Watts
Relative Toughness	Resilient, Elastic	Brittle	Elastic

Table 1.1 Comparison of smart materials. (6,7,10,14)



These numbers are the extreme for piezoelectric polymers at the moment, and are not common for polymer films, but the potential advantage that piezoelectric polymers have over other smart materials is remarkable. The cost saving in power consumption and manufacturing is enough to warrant more extensive research. In addition, the piezoelectric voltage coefficient of PVDF is, on average, 20 times greater than the more common ceramic crystals. The piezoelectric constants for PVDF are shown in Table 1.2. Also listed below, in Table 1.3, is a comparison of the piezoelectric constants of some common ferroelectric materials. The negative values associated with the piezoelectric constants of polymers are due to Poisson's ratio, or the relationship between the compression of the material in the thickness to the expansion of the material in the plane direction ^(6, 7, 14, 15).

Piezoelectric Strain (pC/N)	$d_{31} = 21$	$d_{32} = 2.3$	$d_{33} = -26$	$d_{24} = -27$	$d_{15} = -23$	
Compliance ($10^{-10} \text{m}^2/\text{N}$)	$s_{11} = 3.65$	$s_{22} = 4.24$	$s_{33} = 4.72$	$s_{12} = -1.92$	$s_{23} = -1.92$	$s_{13} = -2.09$

Table 1.2 Piezoelectric coefficients of poly(vinylidene fluoride). (6, 7)

Material	Piezo Constant (pC/N)	Piezo Strain/Volt ($\text{Vm}/\text{N} \times 10^{-3}$)
BaTiO ₃	191	12.6
Quartz	2.3	50.0
PZT-4	289	25.1
PVDF	-33	-339

Table 1.3 Piezoelectric constants for some well know materials. (14, 15)

1.4 Applications of Piezoelectric Polymers

Piezoelectrics have been used to sense forces, deformation, and changes in temperatures. These devices have been incorporated into systems where the data they collect are used to control how they respond to their environment. There are forms that can directly or indirectly control their response to environmental changes and are now being incorporated in smart structures. Smart structures incorporate actuators, electromagnets, controllable fluids, etc, to adjust to their surroundings. The main advantages with piezoelectric materials in smart structures are that they sense micrometer level displacements at high frequencies and use little power for actuation ^(1, 8).

Piezoelectric polymers are extremely useful in monitoring vibrations and in controlling flexible structures. Not only can they be used to measure the extent of deflection and



frequencies of vibration, they can also control the structure through actuation. Piezoelectrics in general can be bonded to surfaces or can be embedded within structures. Using multiple layers of PVDF, one of its copolymers, or another piezoelectric polymer, it is possible to sense the vibrations in one layer and control the vibration with another.

The advantage to using a piezoelectric polymer for vibration damping is that the polymer already provides some damping. A piezoelectric polymer can damp vibrations passively and as the need arises, the stiffness of a material can be changed with an applied electric field enhance damping effects ^(16, 1, 8).

Previous research showed PVDF's usefulness as a sensor in the vibration damping and motion control of dynamic structures. The mechanical properties are time, pressure, and temperature dependant while the piezoelectric response is not. This allows PVDF to maintain its inherent damping capacity without sacrificing its piezoelectric response due to changes in the surroundings ^(11, 15). Date and coworkers realized the potential of PVDF in acoustical damping and induced changes in elasticity by exciting the samples with vibrations and used the potential created by the piezoelectric effect to induce a change in the material ⁽¹⁷⁾.

Research has been conducted on polymer actuators to damp out small vibrations in weightless environments. Such experiments focused primarily on the actuation response on piezoelectric polymers. On a larger scale and in a more practical environment, polymers could damp out vibrations by actuation and through an active change in elastic modulus. Research has also been conducted on composites of piezoelectric materials, particularly PVDF and ceramics, to combine the best properties of both materials ⁽¹⁶⁾.

1.5 Properties of Poly(vinylidene fluoride), PVDF

PVDF is typically a semicrystalline polymer that is approximately 50% amorphous. It is most commonly synthesized through the free radical polymerization of 1,1-difluoroethylene. The medium for synthesis is usually water with peroxy compounds acting as the polymerization catalysts. The structure of the monomer is -CH₂-CF₂-, and the chains occur mostly in a head to tail configuration. The molecular weight of PVDF is typically between 60 and 70 kg/mol ⁽¹⁵⁾.

As with most polymers, the mechanical, rheological, and electrical properties of PVDF have been extensively studied. Most investigations focus on two properties of particular importance. The first is the polymer's polymorphism, and second is PVDF's piezoelectric



properties. PVDF's ferroelectric properties are what make this polymer so unique. PVDF is considered to have a stronger piezoelectric response compared with other polymers and is considered easy to process into films ^(6, 19, 20).

Other than its piezoelectric properties, poly(vinylidene fluoride) is a useful polymer due to its chemical stability, resistance to organic solvents, and high elastic modulus compared with other polymers. PVDF has shown to be very useful as a dielectric because of its high permittivity and dielectric strength and low dissipation factor. Compared to other polymers and other piezoelectric materials in general, PVDF has many benefits; some of its more important properties are listed below ^(6, 19, 20, 22):

- High rigidity, resists deformation
- Low glass transition temperature (no transitions between -45° and 170° C)
- Wide range of processing temperatures (185° – 250° C)
- Resistance to heat and combustion
- Resistance to ageing
- Resistance to abrasion
- Chemically inert.
- Non toxic
- Chemically resistant (highly polar solvents will cause slight swelling)
- Stability to radiation (UV, X-ray, Gamma)
- Excellent electrical insulator
- High Curie point (103° C, valuable for high temp piezoelectric applications)

PVDF is the leading piezoelectric polymer because of its well-characterized properties. Commercially available piezoelectric films are created by mechanically drawing and polarizing extruded sheets. The extruded films are stretched on calendaring rolls as they cool, while being simultaneously polarized using strong electrical fields. The molecular structure of resulting films is well oriented to concentrate the piezoelectric effect uniaxially or biaxially depending on the drawing conditions. Because the response to an electric potential acts along the polymer backbone, the more molecular orientation that can be produced in the films, the stronger the piezoelectric response ^(6, 15).



1.6 Stable Polymorphism of PVDF

Researchers have identified at least four different crystals structures for PVDF polymers. By studying the mechanisms and conditions under which these crystal structures form, insight has been gained into the formation of crystal structures in a range of other polymers. The four crystal phases are referred to differently depending on the authors, but the most common naming scheme is α , β , γ , and δ ^(12, 19, 22).

PVDF's α phase occurs in a trans-gauche-trans-gauche (TGTG) formation. This formation, as seen in Figure 1.1, is not a helical or a planar zigzag but a combination of the two. Either a series of G or TG would represent a purely helical structure. The G's represent the bonds that skew the carbon backbone from the plane. Each G or G- bond represents a 60° or -60° angle respectively from the plane of the last bond. A structure containing repetitions of G's or G-'s would have a right or left hand helix. While structures with an alternating G and G- create an incomplete helix that changes direction with alternating G bonds ^(23, 24).

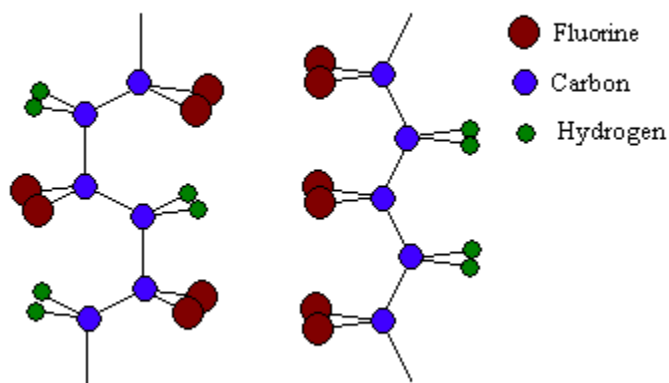


Figure 1.1 Structure of α PVDF (left) and β PVDF (right)

Side group repulsion and crowding are responsible for the semi-helical nature of the PVDF backbone. The helical molecular shape is much lower in energy than the planar zigzag formation, which is most likely why the α phase forms from the melt. Although α is said to be the most chemically stable phase of PVDF, the other phases are also considered stable.



Because of the van der Waals forces acting between the atoms along the carbon backbone and between the molecules of the polymer, the β phase has actually more intermolecular stability while the α phase is favored on an intramolecular basis. These van der Waals forces govern the structure of PVDF and make the trans-gauche-trans-gauche structure of the α phase more stable because of the greater amount of space between the atoms ^(7, 10, 23, 25).

The β crystal phase of PVDF forms a planar zigzag, or TT where T represents a trans bond that remains in the same plane as the carbon backbone. The all-trans structure of β phase PVDF forces the fluorine atoms along the carbon backbone to come closer together and overlap their van der Waals radii. The simple head to tail organization and planar zigzag structure creates a very organized crystal. This structure allows tighter packing density and reduces the intermolecular strain allowing greater chain movement. This crystal structure also allows more dipolar alignment giving the polymer its strong piezoelectric properties ^(7, 10, 19, 23, 24).

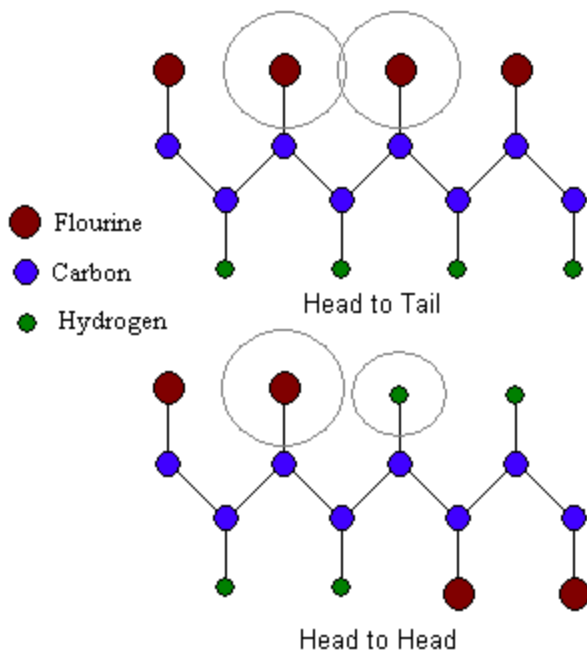
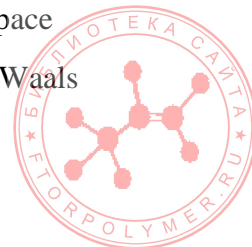


Figure 1.2 The circles around the atoms represent the van der Waals forces between the atoms along the carbon backbone. The distance between the atoms of a head to head configuration have more space between the atoms.

The amount of head-to-head or tail-to-tail monomers along the backbone determines how easily the β phase will form. These imperfections along the carbon chain allow more space between the fluorine atoms and make the β phase more stable. The sum of the van der Waals



radii for hydrogen and fluorine is greater than the distance between the atoms, 2.56 Å as opposed to 2.45 Å, so there is little strain between the two atoms. However when two fluorine atoms are adjacent along the carbon backbone, the sum of the van der Waals radii is greater than the space in between, 2.7 Å, creating strain between the two atoms. An example of the van der Waals radii can be seen in Figure 1.2 ^(7, 26).

A certain percentage of these HH or TT defects during polymerization decreases the likelihood of β phase formation. When the percentage of HH and TT monomers are between 10 and 15%, the α and β phases are equal in potential energy and thus β forms more easily. The introductions of copolymers such as tri-fluoro-ethylene and tetra-fluoro-ethylene can take the place of these HH or TT monomers and increase the production of β PVDF ^(7, 26).

The addition of the HH and TT defects reduces sufficient stress to stabilize the crystalline structure without interfering with molecular polarity. Studies have shown that the HHTT units are distributed randomly along the polymer chain. The temperature at which PVDF is synthesized determines the number of head-to-head (HH) and tail-to-tail (TT) units that occur in polymer chains. The percentage of head to head occurring in most commercially available PVDF is approximately 5% ^(10, 21, 26).

The unit cell of the α phase is orthorhombic with dimensions $a=4.96$, $b=9.64$, and $c=4.62$ Å and has a density of 1.92 g/cm^3 . The β phase is also an orthorhombic unit cell with lattice constants of $a=8.45$, $b=4.88$, and $c=2.55$ Å and has a density of 1.8 g/cm^3 . The unit cell dimension of the γ and δ phases are very similar to α , which is expected since the structure of these phases is also semi-helical. Figure 1.3 and 1.4 illustrates the unit cell configuration for α phase and β phase PVDF respectively. Table 1.4 gives the unit cell dimensions and space groups for all four PVDF phases ^(7, 10, 20, 22).



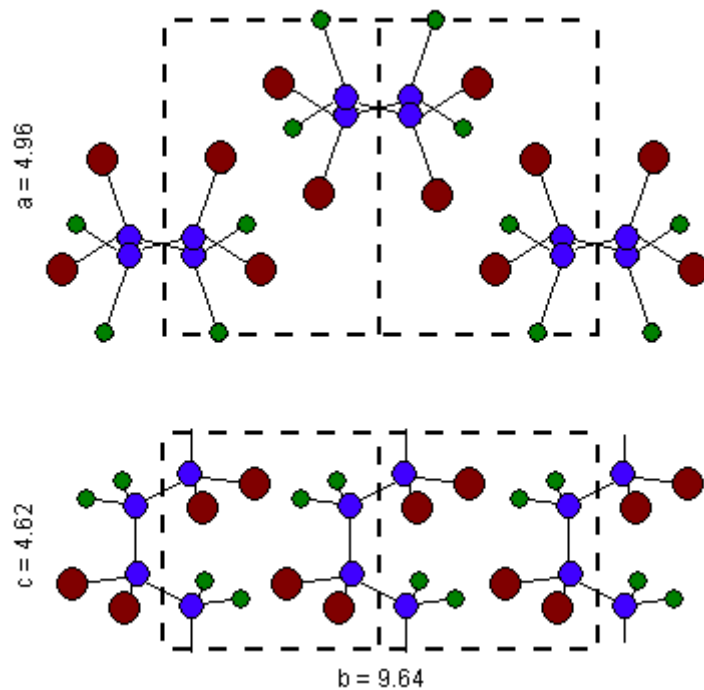


Figure 1.3 Unit cell structure of α phase PVDF.

X-tal Structure	Space Group	a (Å)	b (Å)	c (Å)
α	$P2_1/C$	5.02	9.63	4.62
β	C_m2_m	8.58	4.91	2.56
γ	$C_2C_m, \beta = 90^\circ$	4.97	9.66	9.18
	$C_cC_m, \beta = 90^\circ$	4.96	9.58	9.23
δ	P_{2cn}	4.96	9.64	4.62

Table 1.4 Dimensions of the unit cells for the crystalline structures of PVDF. (7,10)



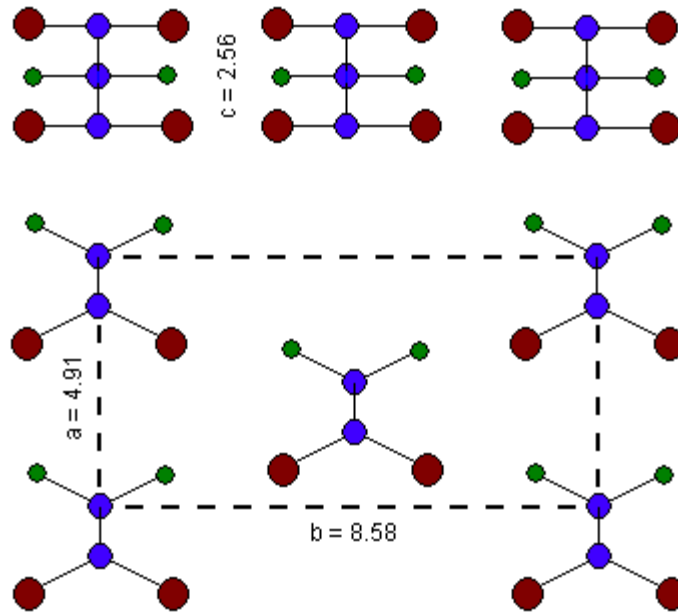
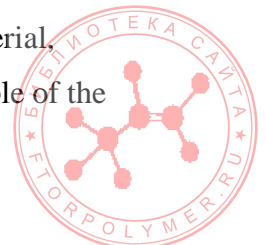


Figure 1.4 Crystalline structure of β phase poly(vinylidene fluoride).

1.7 Poling of PVDF

Each PVDF chain has a coupling of positive and negative charges referred to as a dipole. The negatively charged fluorine atoms are coupled with the positively charged hydrogen atoms or protons. The dipoles are rigidly attached to the carbon backbone and their orientation depends on the polymer crystal structure. This orientation of the dipoles determines which crystalline structures of PVDF are piezoelectric. The β phase has a highly polar arrangement of the hydrogen and fluorine atoms. All-trans structures of the β phase align the charged hydrogen and fluorine atoms and produce a net polarization of the unit cell. The dipoles along the carbon backbone, and within the crystal, align themselves maximizing spontaneous polarization within the unit cell ^(6, 7, 10, 23).

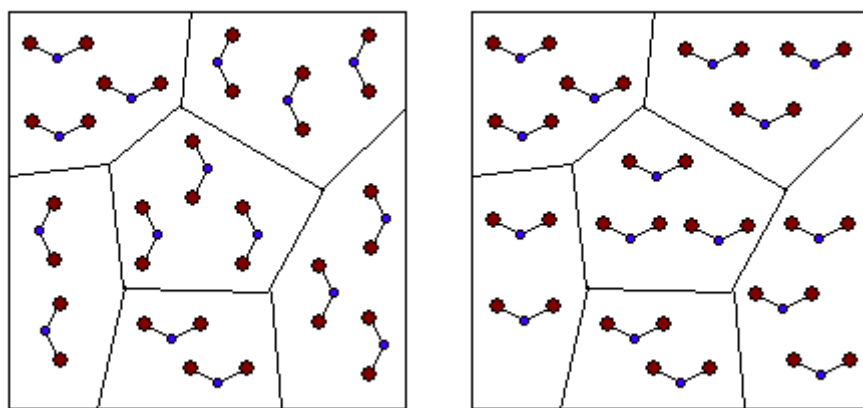
The strong dipole formed by the all-trans conformation of the carbon backbone, and parallel arrangement of the chains in the crystalline unit cell creates a net charge in the β phase structure of PVDF. When β forms naturally the net charge is zero because the dipoles are arranged randomly. However, when a large electric potential is applied across the material, during the manufacture, the dipoles align and produce a net positive charge. An example of the



dipole alignment can be seen in Figure 1.5. This net charge allows the polymer to respond to electrical fields. In contrast, the α phase is electrically inactive because the dipoles are disorganized in the unit cell ^(6, 7, 11, 27, 28, 29).

This dipolar alignment, or poling, must be performed on any piezoelectric polymer before it can be used piezoelectrically. The mechanisms for poling are not very well understood. What is known is that crystals within a polymer are influenced with an electric field to create a net polarization. This net polarization of PVDF aligns the individual crystals within the polymer causing them to collectively respond to changes in their surroundings, and gives PVDF its strong piezoelectric characteristics. Crystalline ferroelectric polymers have a polar unit cell by definition. During poling the direction of this unit cell can be changed when a sufficient electric field is applied ^(7, 11, 27, 28).

Poling processes for PVDF use electric fields in the order of 20MV/m and temperatures around 100°C to convert non-polar β PVDF to its polar form. The degree of polarization is linear with applied voltage until a saturation level occurs. The same polarization response can be achieved at any temperature, but the duration the field must be applied increases at lower temperatures. Poling at lower temperatures (usually below 70°C) can produce a non-uniform distribution within the film. Uniformity is best achieved by applying electric fields for an extended period of time at temperatures above 90°C. The polarized β phase is stable and the decay of polarization is only significant at temperatures above 140°C ^(4, 11, 27, 28).



Random

Aligned

Figure 1.5 Example of the alignment of dipoles within β phase PVDF.



1.8 Phase Transformations

The α phase is the most stable and the most common of the crystalline phases and mainly occurs as a result of crystallization from the melt. The melting point of PVDF is 167°C and at temperatures below 160°C degrees α and γ crystals form. Below 150°C the α phase is the primary structure and above that temperature the fraction of γ phase increases with increasing time and temperature ^(10, 12, 19, 30).

PVDF's relatively simple composition allows high chain mobility and easy conversion from one crystal phase to another. The process schemes to obtain the other three metastable phases from α can be seen in the Figure 1.6. PVDF is highly sensitive to radiation and excessive exposure will damage the crystalline structure of the polymer to the point where is almost entirely amorphous but under controlled conditions irradiation can change the crystal structure and induce piezoelectricity ^(12, 20, 31).

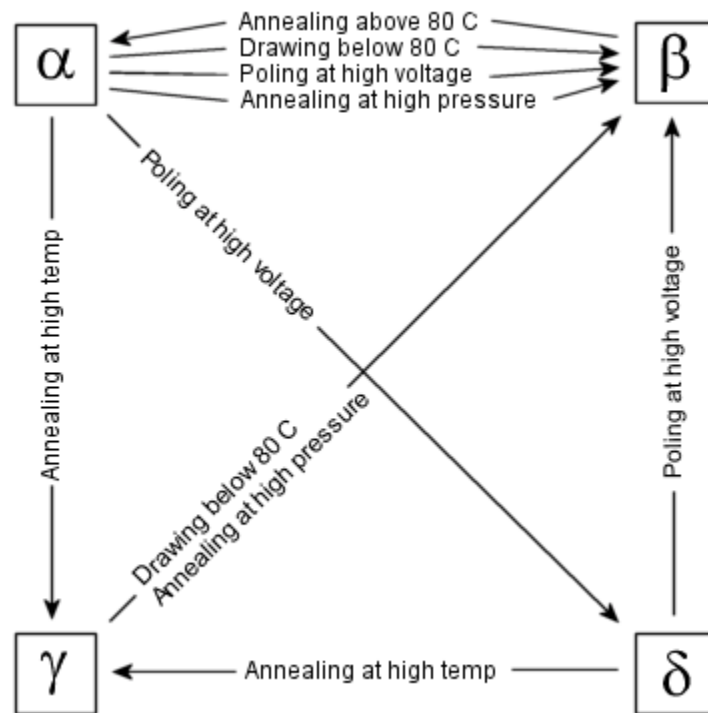
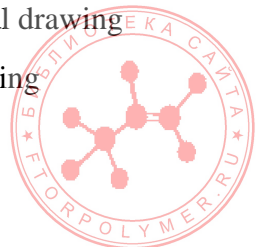


Figure 1.6 Diagram showing how each of the crystalline phases of PVDF can be achieved.(7,10)

The simplest and most effective way to obtain the β phase is through mechanical drawing of the α phase. The β phase forms when drawn at temperatures below 100°C . At drawing



temperatures higher than 100°C, only a portion of the α phase will convert the β phase and at drawing temperatures above 120°C no β phase will form. To convert all the α phase to β a strain of at least 300 percent is needed at a temperature below 100°C^(12, 19, 30).

At temperatures below 80°C the β phase is the most stable. This may explain the formation of the β phase upon drawing. The α crystals are pulled apart during deformation and reform as β crystals due to their higher stability. The β phase is said to form from the melt when quenched to 80°C, however it is extremely difficult to avoid formation of α crystals. β phase PVDF can also be solvent cast from a solution of dimethylformamide or dimethylacetamide. Depending on the temperature of evaporation, the resulting film will be either α or β . Processing at temperatures above 110° C will produce α ; below 70°C will produce β and intermediate temperatures produce a mixture of the two. Obtaining β phase films through solvent casting often produces samples that are not mechanically sound. Both the α and the β phase films can be drawn to produce highly oriented β phase. The β phase has also been obtained using special methods involving crystallizing copolymers from the melt and growing epitaxially on a KBr crystal^(32, 19, 20, 23, 30).

Because drawing is needed to create a piezoelectric film, research on these materials is difficult. Drawing of PVDF film creates irregularities and defects in the film. Even when samples are created free from measurable defects the properties of the films differ from sample to sample and there are always residual amounts of non-piezoelectric PVDF in the film⁽¹⁹⁾.

1.9 Milling

Mechanical milling was first introduced in 1968 to produce nickel-based super-alloys. The process dispersed the alloys components before processing. In metals, alloys can experience phase transformations, and pure metals can become nanocrystalline. A similar technique is used with polymers to combine two polymers that will not mix under normal conditions. This produces solid-state dispersions of polymeric blends that can claim properties unachievable with the individual polymers.^(33, 34, 35, 36)

The mechanisms that affect the fine powders within the ball mill are quite complicated. On a microscopic scale the particles are fractured and deformed. The particles also experience localized area of heat and pressure resulting from the collisions. At these locations melting and



chemical changes can occur resulting in new materials or crystal structures. The polymer chains are cut and reattached due to these violent local reactions, affecting the polymers on a molecular scale. ^(33, 34, 35, 36)

The mechanical milling technique described in this paper uses a high-energy shaker ball mill to mechanically deform and grind materials to produce a fine powder. The powder is continuously fractured, deformed and cold welded over an extended period of time. In most instances the process is used to blend materials, which would otherwise be incompatible, well below their melting temperatures. However, the milling of individual polymers can change the crystal structure.

The technique of mechanical ball milling was shown to produce changes in crystalline polymers by Pan and Shaw ⁽³⁴⁾ as well as Castricum and his coworkers ⁽³⁶⁾. Both groups observed not only a change in the level of crystallinity in their samples but also a change in crystalline structure. Contrary to their findings, Font and coworkers ⁽³⁵⁾ produced polyethylene terephthalate and sucrose in an almost entirely amorphous phase. Overall the results obtained from milling of various polymers and copolymers depend largely on the nature of each polymer. By milling the α phase it may be possible to convert to the β phase without drawing ⁽³⁷⁾.

After milling the resulting powder can be processed in any number of ways but to ensure that the material's crystal structure remains it is necessary to compression mold particles below the melting point under high pressure. Compression molding will not produce the highly oriented polymers found in the purchased films but the β phase will remain intact. An unoriented β phase will not respond to the same extent, but will have an electrostrictive response that could still prove useful. If the β phase could be achieved before processing and the crystalline structure maintained after processing, then piezoelectric samples could be made into a variety of complex shapes and sizes that could be used in a wider range of applications ⁽⁸⁾.



Chapter 2 Experimental Equipment and Procedures

2.1 Sample Preparation

The PVDF powder and purchased piezoelectric films were prepared following the procedures summarized below. The purchased films were prepared following the manufacturer's suggestions. All other samples were prepared based on literature or common processing techniques for polymers.

2.1.1 Hot Pressing films

Bulk PVDF powder, particle size 5 μ m, was purchased from Atofina (www.atofina.com, trade name Kynar® 741). Atofina reports the molecular weight of the powder to be approximately 64 kg/mol with a density of 1.772 g/cm³. Atofina also reports the melting point and glass transition temperature of the Kynar® powder to be 168°C and –45°C respectively. The melting point was confirmed through differential scanning calorimetry, the results of which can be seen in Figure A.14 in the appendix ⁽³⁸⁾.

The α phase of PVDF will form at any temperature regardless of the amount of time it has to crystallize from the melt. This makes it very difficult to obtain samples of PVDF with any of the other three crystalline structures. The ideal conditions to form γ are slightly above the melting point at atmospheric pressure. Test films were pressed from the PVDF powder at 180°C to obtain the γ phase. Lower temperatures will form the α phase or, most likely, a combination of the two. Because of its faster growth rate, the α phase preferentially forms crystals and limits the formation of the other crystal phases.

Sample films were made from the Kynar® powder with a Carver hot press. To create films of different crystalline structures various combinations of heat, pressure, and quenching were used. The different combinations are summarized in the experimental matrix, Table 2.1. All films were pressed for 60 minutes.



Quenched	Unquenched
180°C and 2000lbs	180°C and 2000lbs
220°C and 2000lbs	220°C and 2000lbs
180°C and 20,000lbs	180°C and 20,000lbs
220°C and 20,000lbs	220°C and 20,000lbs

Table 2.1 Temperature and pressure combinations of pressed PVDF films.

Films manufactured at higher temperatures and pressure allow for other crystalline phases to form other than the α phase. All quenched films were immersed in liquid nitrogen upon removal from the hot press to retard crystallization.

Powder samples compression molded at 20,000 lbs (800 psi), at either 180°C or 220°C, and quenched were cold drawn to 300% elongation to simulate the drawing process performed on the commercially available films from Measurement Specialties (www.msiusa.com, Norristown, Pennsylvania). Films were drawn with the TA-XT2i Texture Analyzer (Stable Micro Systems, Surrey, United Kingdom). Each sample was drawn at a 0.1 mm/s deflection rate until the sample reached 300% of its original length, and then held in the elongated state for approximately 30 minutes to reduce elastic recovery.

2.1.2 Mechanical Ball Millings

The ball mill used in this experiment consisted of a stainless steel sample container and 10 small stainless steel balls. The balls were approximately 1 cm in diameter. The canister stroke (travel) was fixed and measured to be about 3 inches (76.2 mm). The mill operated at a rate of 450 to 500 rpm, which equates to approximately 7.5 to 8.3 strokes per second. A schematic of the ball mill can be seen in Figure 2.1.



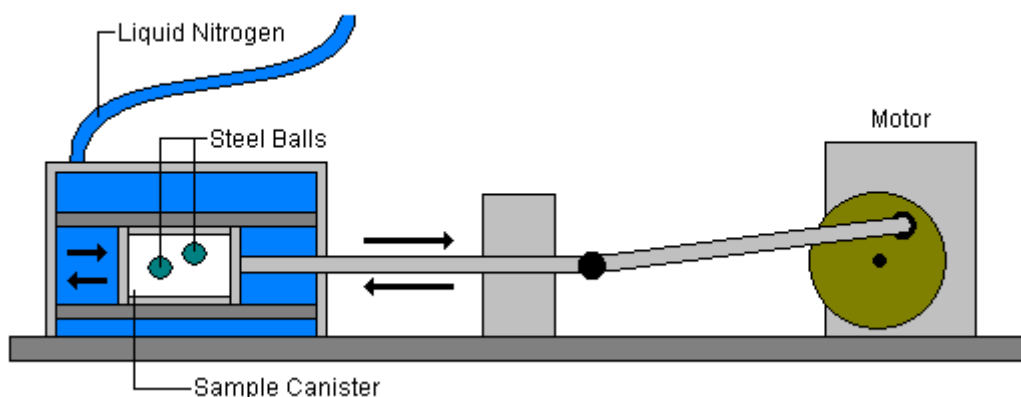


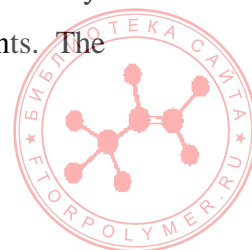
Figure 2.1 Diagram of shaker ball mill used during mechanical milling of Kynar® PVDF.

To maximize milling effectiveness the canister was cooled to below PVDF's T_g using liquid nitrogen. The cooling of the ball mill kept the Kynar® powder in a very brittle state where the maximum amount of fracture and deformation could occur. Samples were milled for 1.5, 4 and 8 hrs. After which the PVDF powder was removed and compared to the original sample using x-ray diffraction. The milling times were chosen based on the results of the previous run and the desired results that were to be obtained.

2.1.3 Preparation of Purchased films

Pre-fabricated films were purchased from Measurement Specialties (Norristown, Pennsylvania), a producer of piezoelectric PVDF films for use as sensors and actuators. The films were obtained in three thicknesses: 28, 52, and 110 μm and in two different size sheets: 5 x 8 and 8 x 11 inches. The sheets came with or without electrodes already fixed to each side that can be used to attach electrical leads. The electrodes consist of either silver or nickel based paint silk screened to form a thin layer on each side of the films. The application of the electrodes can be obtained in a variety of standard patterns or special ordered depending on the design of the final device.

For the purpose of these experiments, the films were purchased in the 5 by 8 inch (127 by 203 mm) configuration and in each available thickness. Different film thicknesses were required for different experiments. The silver electrodes were chosen because their increased flexibility and decreased thickness would minimize the effect of the electrodes on the measurements. The



silver electrodes were 7.5 μm thick and were purchased covering the entire sheet so samples could be cut to any desired size or shape.

Before cutting the samples to size, the silver electrodes were stripped off the sheets along the cut lines. Common masking tape was laid down over top of the electrodes to be kept and the silver paint was stripped off elsewhere using acetone. This method ensured that the electrodes, on either side of the film, did not short together when cut. A short between the two electrodes would eliminate the electrical potential necessary to activate the piezoelectric response. After the samples were cut, the edges were cleaned thoroughly with acetone and tested for short circuits using a Fluke (Everett, WA) multi-meter. As a quality check the presence of shorts between the two electrodes of each sample were measured. A short was measured as a current flow from one electrode to the other. Those samples with infinite resistance between the electrodes were considered acceptable.

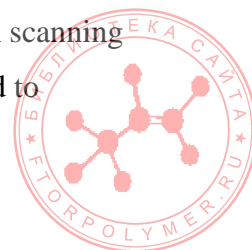
To prevent short circuits on the testing equipment that may interfere with results or damage equipment, each sample was prepared so that only the unpainted surface of the film would contact the subsequent testing rigs. The silver paint was only allowed to remain on those surfaces that did not come into contact with the test apparatus.

2.1.4 Annealing β Phase PVDF Films

The purchased films were annealed starting at either 80 $^{\circ}\text{C}$ or 150 $^{\circ}\text{C}$ to examine the effects of annealing on the crystal structure. Because of the highly oriented nature of the purchased films, samples were annealed in a hot press to minimize the retraction that can occur with freely annealed films. Annealing the β phase at temperatures below 80 $^{\circ}\text{C}$ will not affect the crystal structure unless the annealing occurs over extremely long periods of time, months or years. However, at temperatures above 80 $^{\circ}\text{C}$, the crystal structure is less stable and may transform to the α or γ phases. By observing the effect of elevated temperatures on the crystal structure of PVDF film, the conditions of β phase instability can be determined⁽³²⁾.

2.2 Material Characterization

The compression molded films and the purchased films were characterized with scanning electron microscopy (SEM) and wide-angle x-ray diffraction (WAXS). SEM was used to



observe changes in size and texture of the milled and unmilled Kynar® powder as well as the quality of the sintered PVDF films. X-ray diffraction was used to determine changes in crystal structure due to milling or annealing of PVDF powders and films.

2.2.1 Wide Angle X-ray Diffraction (WAX)

To characterize the crystal structures of the Kynar® powder, prepared films, films from Measurement Specialties, and annealed films a Scintag XDS2000 X-ray Powder Diffractometer (Ecublens, Switzerland) was used.

A continuous scan was performed on the XRD with 2θ angles ranging from 5 to 70 degrees and a chopper increment of 0.04 degrees. Powder samples were rotated to ensure that the crystal structure was measured regardless of the particle orientation. Rotating the films did not show any changes in the measured crystal structure. A sample of virgin PVDF powder or purchased film was scanned with each set of samples to evaluate any baseline shift in the XRD.

2.2.2 Scanning Electron Microscopy (SEM)

Scanning electron microscopy examined the surfaces of the powders and films to observe the size and shape of powders after milling and to examine the quality of films after sintering. The apparatus used for imaging was a SI-SX-40 Scanning Electron Microscope. The Kynar® powder, as received, and milled powder were deposited on double sided tape to hold them in place. All samples were coated with an approximately 300 Å thick layer of gold in an Edwards S150B sputter coater. Magnifications of 1000x and 8000x were used to view all powder samples. Because of the texture of the particles, 8000x was the highest magnification in which the microscope could be focused. Magnifications of 1000x and 10,000x were used to view the sintered films. Particle size determination was done qualitatively by taking an average of the particles viewed in the electron microscope.

2.3 In-Situ Mechanical Testing

In-situ mechanical testing was performed to evaluate the viscoelastic properties of PVDF thin films under different applied voltages. Creep testing was used to evaluate the stiffness of



the films while dynamic mechanical analysis examined the changes in storage and loss modulus. These procedures are outline below.

2.3.1 In-Situ Creep Testing

Creep tests were performed to analyze the change in overall stiffness of PVDF when subjected to different electrical potentials. A change in elastic modulus can impact the material's performance when used in actuation or damping devices. Sample creep was measured with a TA-XT2i Texture Analyzer. In this experiment, the unit was programmed to load the test samples, in tension, with constant force and to hold that force for 10 minutes. The Texture Analyzer recorded the force, displacement, and strain with respect to time.

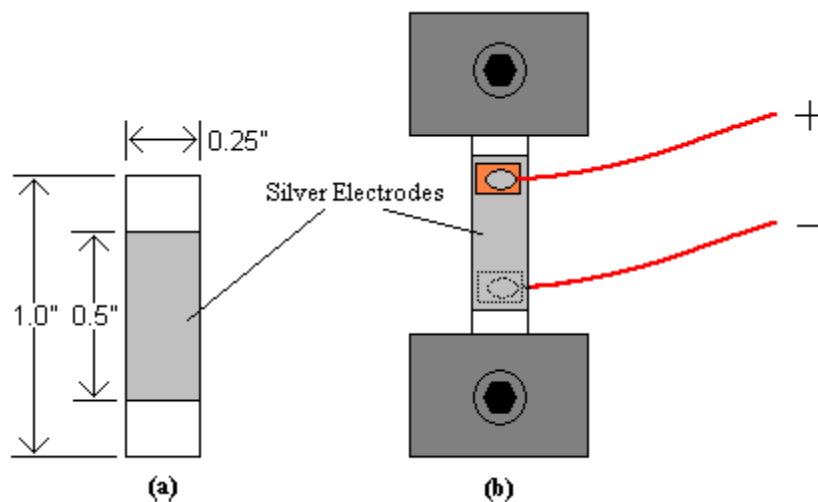
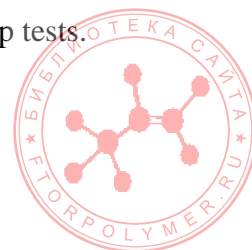


Figure 2.2 (a) Dimensions of the creep samples and (b) a diagram of the creep experiments.

The clamps of the Texture Analyzer were lined with 400-grit sandpaper to prevent sample slippage and to distribute the force of the retaining clamps more evenly over the area. This reduced the stress concentrated at the top and bottom of the retaining clamps. The samples were fixed into the clamps so that only the silver electrodes on either side of the sample were exposed as shown in Figures 2.2 and 2.3. This ensured that only biased PVDF would be in tension during the test procedure to maximize the piezoelectric effect. The first PVDF samples were pulled in tension until failure. Based on the ultimate tensile strength of the sample, a load of approximately 75% of the measured stress at failure was used for the remaining creep tests.



The samples were cut with the dimensions shown in Figure 2.2 using the 110 μm thick PVDF samples. All samples were loaded in the direction of orientation and were biased with a range of voltages by attaching wires to the electrodes with copper tape. Wires were soldered to the tape, which is conductive through the adhesive. A minimal amount of copper tape, approximately 2 mm in diameter, was used to minimize any effect the tape might have on the experiments. Although these connections were temporary, there were no indications that the connections influenced the measurements.

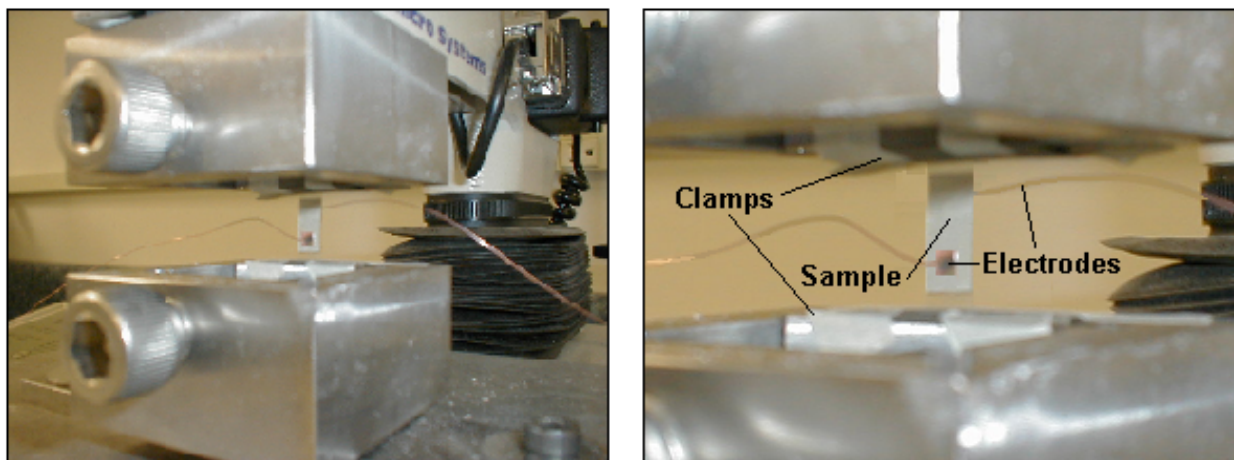


Figure 2.3 Sample of PVDF film with wires attached, clamped into the Texture Analyzer.

The PVDF films were subjected to a range of voltages from 0 to 50 V DC (0 to 1 V/ μm) in increments of 10 V. For each voltage, a set of six samples were used and subjected to a constant load of 100 N, corresponding to a stress of 303 MPa. To measure the extent the piezoelectric forces had on the experiments, loads were reduced in an additional experiment. These tests used a reduced load of 50 N at 0, 10, and 60 V. Electric potential for all experiments was provided by either a 0 to 60 V Avionics or a 0 to 20 V DC Hewlett Packard DC power supply.

Annealed samples were also tested, using the same load and voltages, to measure the effect of subjecting PVDF to high temperatures. Additional samples were pulled perpendicular to the direction of orientation to compare the response to a normally applied force.



2.3.2 In Situ Dynamic Mechanical Analysis (DMA)

Dynamic Mechanical Analysis, DMA, tests were performed with a Perkin Elmer DMA7 Dynamic Mechanical Analyzer (Wellesley, MA). The first sets of tests were performed in the three-point bend configuration. The samples used were the same size and shape as those in the creep tests, but the ends were removed so only the silvered covered portion remained. The samples were also tested perpendicular to the direction of orientation instead of parallel like the creep tests.

Only 110-micron samples were used due to the added stiffness requirements to produce consistent results in three-point bending. Thinner films could not sufficiently support the weight of the probe to provide acceptable test data. Frequency scans were used to analyze the materials response to an applied load at a range of frequencies from 1 Hz to 51 Hz. The load applied to these samples was 10 mN and 8.3 mN for static and dynamic forces respectively. These forces resulted in initial amplitudes between 8 and 12 micrometers, which are within the range recommended in the owners's manual. All experiments were conducted at room temperature (approximately 20 °C). Bias voltages of 0, 10, 20, and 30 V DC were applied to the samples during testing. This equates to fields of 0, 0.09, 0.18, 0.27 V/ μm .

Because the samples must be allowed to move freely underneath the probe, electrodes could not be attached directly to the sample for fear that they would affect the measurements. Instead the electrodes were attached directly to the stand and the probe where the sample would contact the frame. Although the potential was applied indirectly to the sample, the potential could be measured when wires were attached to the films electrodes. Figure 2.4 is a schematic of the electrode setup and Figure 2.5 shows a photograph of the actual apparatus.



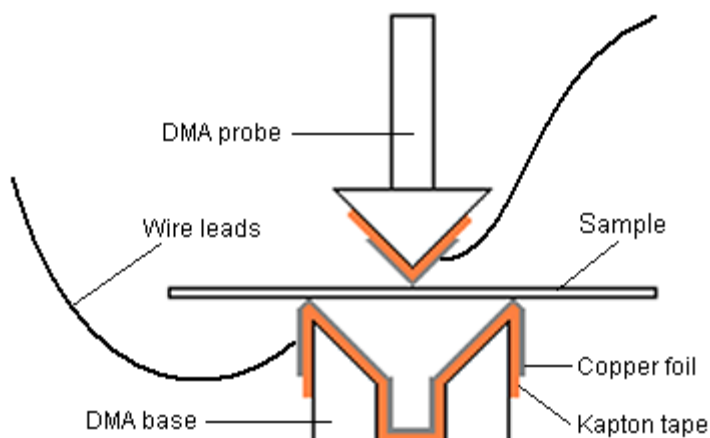


Figure 2.4 Diagram of three point bend setup used in the Perkin Elmer DMA.

Since the probe and base are metallic and the equipment sensitivity to electric currents was unknown, the equipment was isolated from all electric potentials. Having the apparatus directly contact the electrodes would not only short the film but would potentially damage the equipment. To solve this problem, the DMA base and probe were insulated using Kapton® film. The Kapton® tape was tested prior to use to be sure it would withstand the maximum 60 V potential between the probe and base. Kapton® tape was also applied to the sides of the instrument to protect any metal surface from contacting with the wires.

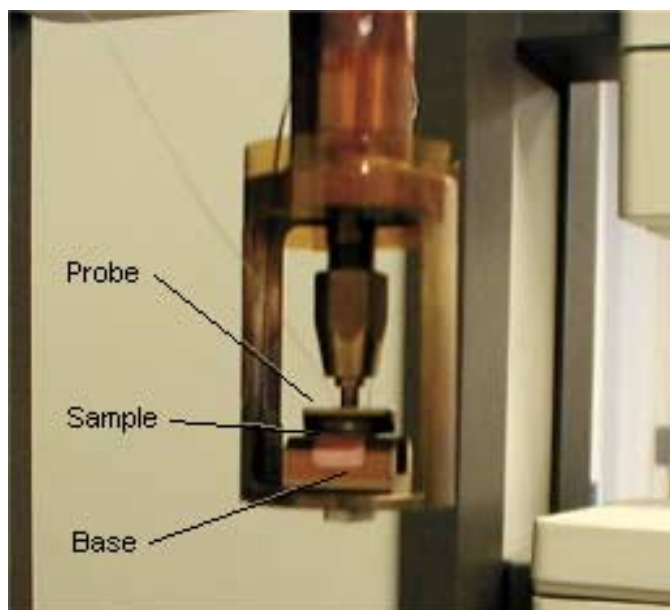


Figure 2.5 PVDF film in three point bend with electrodes attached.



Initial tests were conducted comparing the setup to one without the Kapton and wires connected to the equipment. After reducing the size of the wires and providing sufficient slack in the wire to avoid tension on the probe, the experimental setup showed minimal influence on the measurements.

A second series of tests were performed with the DMA in extension mode instead of bending mode. Extension tests were also performed with a frequency scan and the samples were placed under tension much like in the creep tests. Samples of the purchased PVDF were tested under biased conditions of 0, 5, 10, 20, 30, and 60 V DC (0, 0.18, 0.36, 0.71, 1.07, and 2.14 V/ μm), while a static force of 400 mN and a dynamic force of 333 mN were applied to the sample. The resulting amplitudes were between 5 and 8 micrometers. Since PVDF is fairly stiff, it was necessary to apply such high forces in order to obtain measurable amplitudes.

The samples used in extension tests were cut from 28 μm sheets to the dimensions shown in Figure 2.6. Thinner films were used in these tests to reduce the amount of force required to produce measurable amplitudes. The electrodes were attached to the samples in the same method as the creep experiment and the samples were in tension in the direction of orientation. Once again all metal parts that had potential to come into contact with the wires were insulated with Kapton® tape. The setup, including sample, is seen in Figure 2.7.

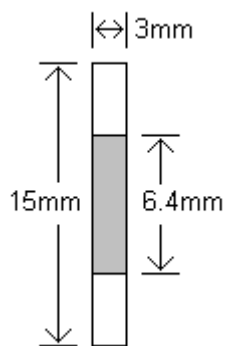


Figure 2.6 Dimensions of samples used in extension in the DMA.



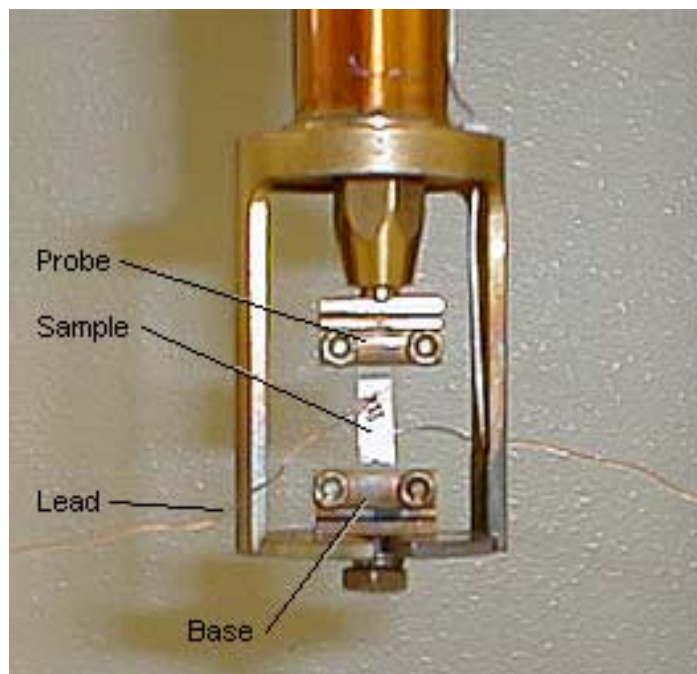


Figure 2.7 PVDF sample in extension with electrodes attached.



Chapter 3 Results and Discussion

3.1 Sample Preparation

The creation and preparation of samples contributed heavily to the quality and consistency of the results. There was much trial and error, especially in attaching electrodes, to create samples that worked well in the various experiments. Hot pressed films were important in determining what crystal structures could be obtained through various combinations of temperature, pressure, and cooling rates. The techniques that produced the best results are outlined in this paper.

3.1.1 Hot Pressing Films

Hot pressing the films resulted in an opaque appearance regardless of the processing time, temperature, or cooling rate. In contrast, the purchased samples were nearly transparent. Since the purchased films were documented to be 50% crystalline and highly oriented, the hot pressed samples may have had a higher level of crystallinity, or contained minute flaws or impurities in the film which were introduced by the hot press process.

3.1.2 Preparation of Purchased films

Punching the mechanical test specimens into the standard “dog bones” shape with the process punch was unsuccessful. The thin, flexible PVDF films deformed around the edges of the punch and samples were often damaged before they could be separated from the sheet. Cooling the samples below their glass transition temperature may have been a solution to this problem. However, simply cutting the mechanical test specimens with a razor blade proved to a quick and easy alternative method and avoided a more complicated process, which could have introduced additional process errors.

The only experiment in which dog bones could be used was the creep testing on the Texture Analyzer. However, since a bulk change in modulus was the desired result from the experiments, breaking the samples was undesirable and avoided greatly. The influence of stress concentrations in a shape other than a dog bone would be minor and most likely not have an



effect on the measurements. All samples were cut with a razor blade, after the silver was removed, using a metal template to ensure consistent size and shape.

3.2 Material Characterization

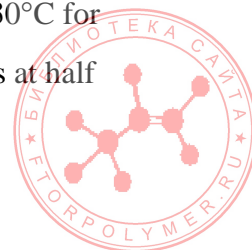
3.2.1 Wide Angle X-ray Diffraction (WAX)

The x-ray diffraction plots for the different crystalline phases of PVDF are easy to distinguish from one another as long as only one crystalline phase exists in the sample. Shown in Table 3.1 below are the crystal planes that have the largest contribution to the diffraction patterns. The different crystal structures have similar peaks, however each phase has one or two peaks that make them easy to identify. The most prominent peak for all of the phases occurs at approximately 20°. The α and γ phases both have a second peak at 18° which makes them easy to distinguish from the β phase. Table 3.1 lists the more prominent peaks observed in PVDF's x-ray diffraction plots.

Alpha		Beta		Gamma	
x-tal plane	2 theta (°)	x-tal plane	2 theta (°)	x-tal plane	2 theta (°)
100	17.7	110	20.8	020	18.5
020	18.4	200	20.7	002	19.2
021	19.9	020	36.6	110	20.1
111	27.8	101	36.6	101	20.3
200	35.7	221	56.1	022	26.8
002	39			200	36.2
022	57.4			211	38.7

Table 3.1 Crystal planes of PVDF's crystal phases and their corresponding 2 theta peaks.

Annealing the purchased films examined the robustness of the β phase and its ability to endure heat and pressure during processing. The x-ray results of the purchased films produced peaks that were characteristic of the β phase crystals. The most prominent peak was a reflection representing (110) and (200) crystal planes, occurring at a two theta angle of 20°. After annealing the purchased films for one hour at 80°C, an 11% decrease in crystalline diffraction was observed in the peak at 20°, which can be seen in Figure 3.1. After annealing at 130°C for one hour a decrease of 52% occurred in the main peak at 20°. The widths of the peaks at half



intensity increased by 0.3° and 0.5° for the films annealed at 80° and 130° respectively. A shoulder appeared next to the main peak after annealing suggesting a decrease in orientation and perhaps the conversion to the α phase crystal structure. The appearance of the α phase in the annealed samples indicates that β phase PVDF cannot be processed above 80°C and retain its crystalline structure. This finding is consistent with literature stating the α phase is the most stable above 80°C ^(10, 24). Samples annealed in an oven significantly shrunk in physical size with relaxation as compared to the sample annealed in a hot press. However, their x-ray diffraction patterns were the same suggesting no difference in crystallinity. When annealed at high pressures, 400 psi or more, and at temperatures below 80° , no changes in crystallinity or orientation were observed.

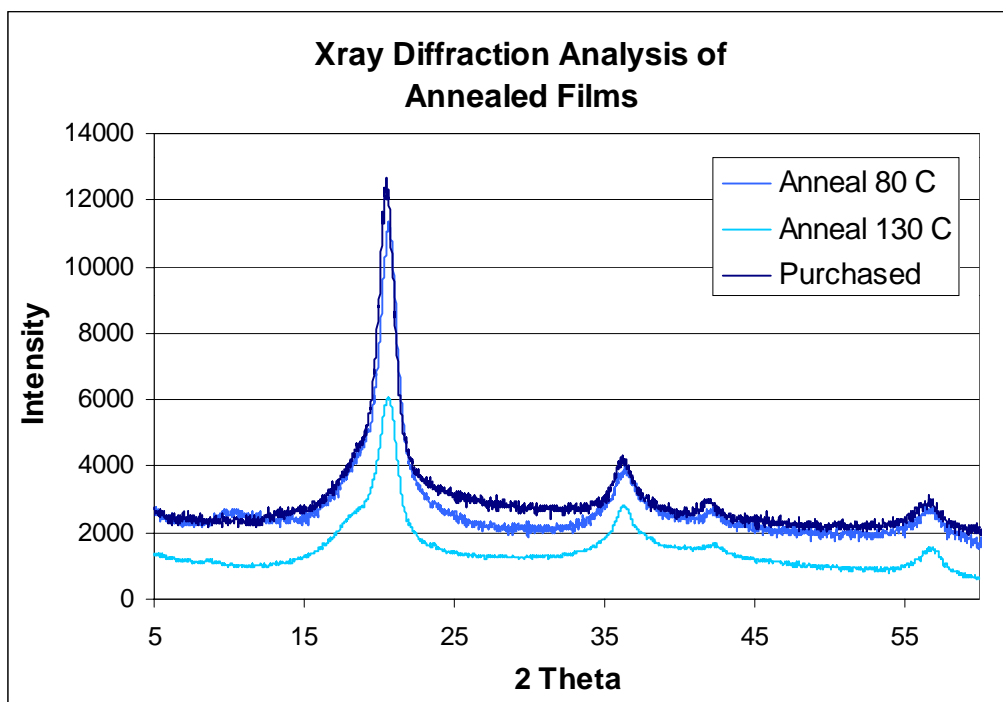


Figure 3.1 X-ray analysis of annealed purchased PVDF samples. Samples were annealed for 1 hour.

The initial x-ray results of the Kynar® powder showed peaks associated with a combination of both α and γ phase crystals. A dual peak caused by the (020) and (021) crystal planes is characteristic of the disordered semi-helical structure that would occur in the α phase. Researchers Gregorio and Xu both observed these peaks as well as a smaller peak at 17.7° ^(19,20). This third peak is seen in Figure 3.2 as a shoulder in the (020) peak at 18.4° . The crystal



structures of the α and γ phases had similar diffraction plots making it difficult to distinguish between the two. However, a peak occurring at a 2-theta angle of 57° is unique to the (022) crystal plane of the α phase. The observed peaks were very small as compared to those of the purchased films suggesting lower crystallinity and/or significantly less orientation, which would result in a much lower observed piezoelectric response.

Examination of the diffraction results of the pressed films, revealed no combination of temperature, pressure, or cooling rate, which would yield the β phase crystalline structure. Also the x-ray results did not indicate a combination of temperatures or pressures that would produce a pure α or γ phase structure. Instead the results, shown in Figure 3.2, reflected a combination of α and γ phase crystals that show only minor effects of the processing variables. The peaks of the x-ray results were greater in intensity than those of the original Kynar® powder, which would suggest an increase in the crystallinity or possibly some orientation of the crystals due to the pressure of the hot press. It was expected that PVDF would produce the γ phase when formed at high temperatures and perhaps form the β phase at high pressures^(12, 20, 31). However, no such results could be produced. It was also expected to produce amorphous samples by quenching but only a slight decrease in crystallinity was obtained. As can be seen in Figure 3.2, the quenched samples exhibited only a 9% decrease in crystallinity when compared to the films cooled slowly under ambient conditions. Gregorio and Cestari⁽³⁰⁾ also observed these complications when processing PVDF. They were also unable to produce β phase from the melt, observed the γ phase forming quite readily with the α phase, and were also unable to avoid crystallization by quenching. Gregorio and Cestari indicated they could produce the α phase by itself through quenching. However, this study protocol could not reproduce these results.



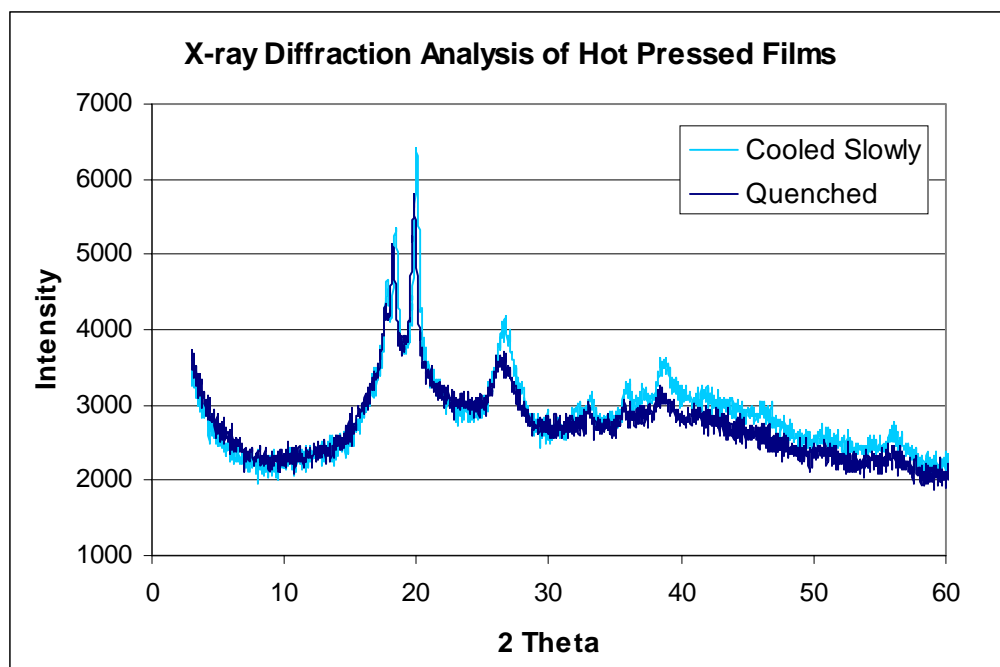


Figure 3.2 X-ray analysis of hot pressed films. Films produced identical results regardless of the conditions in which they were made.

After determining that all of the hot pressed films produced the same results, two samples were chosen for cold drawing. Both films were made at high pressure but one was pressed at 180°C and the other at 220°C. The films made at higher pressure, 800 psi with the hot press, were thinner and were easier to cold draw without damaging them. The diffraction results of these two samples were the same and produced the β phase crystal structure as shown in Figure 3.3. Upon drawing, the samples became cloudy and showed a 9% increase in the intensity of the diffraction peaks compared to the samples before drawing. This increase due to strain induced crystallization and/or orientation of the films. The hot pressed films, which were mostly α , transformed to mostly β phase upon drawing. This was to be expected as drawing the α phase has proven to be the only way to consistently produce β PVDF samples that are structurally sound. The phase composition obtained from drawing is seen in the diffraction patterns in Figure 3.4 as the double peak of the α phase has combined into one peak at a 2-theta angle of 20°. Purchased films produced a 60% increase in peak intensity at a 2-theta angle of 20° contributed to their higher levels of crystallinity and orientation.



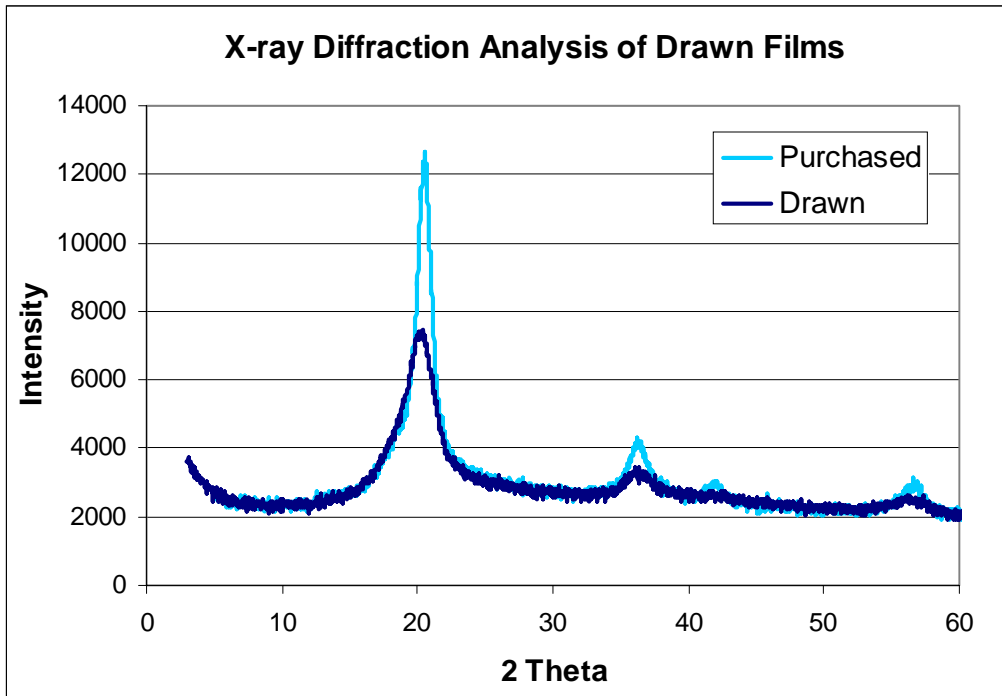


Figure 3.3 Comparison of purchased and drawn films. The drawn films showed the same crystalline structure as those purchased from Measurement Specialties.

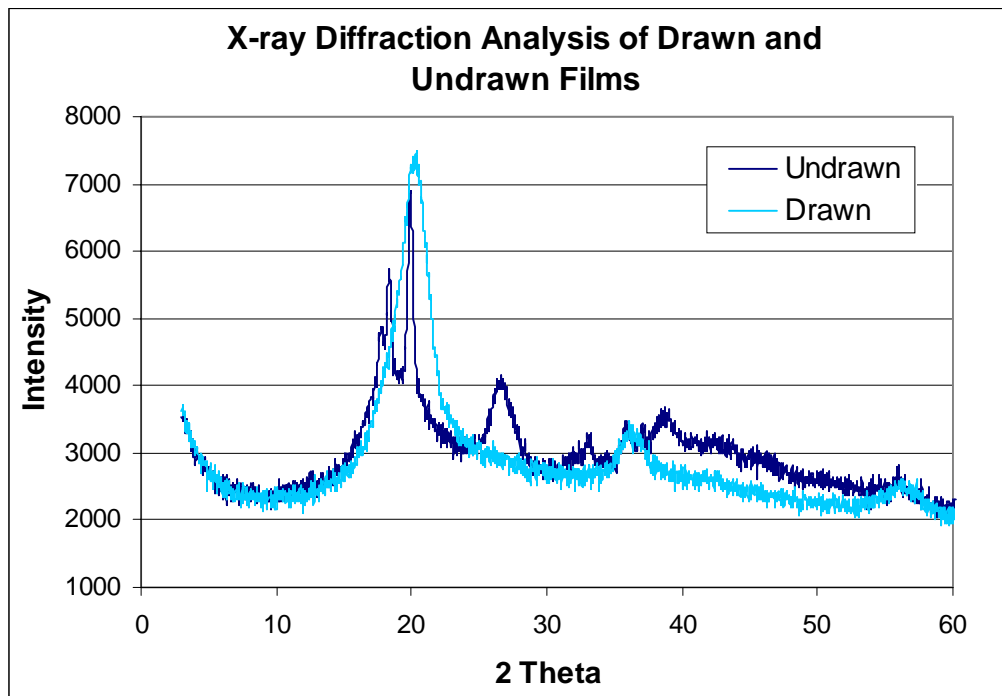


Figure 3.4 Comparison of drawn and undrawn films. Both samples were cut from the same sheet before one was drawn.



The diffraction results of the milled PVDF powder showed a change in crystallinity associated with the milling. There was no significant increase in the degree of crystallinity but small changes in the phase of crystallinity was indicated by the shift from the α/γ phase to the β phase as shown in Figure 3.5. The phase shift of the milled Kynar® powder is evident by the shift in the location of the peaks. The α phase has two main peaks around 18° and 20° where the β phase has only one peak. The diffraction results of the milled samples showed some of the smaller peaks diminishing as well as one of the higher intensity peaks. The diminishing of the smaller peaks also suggests a conversion from the α to the β phase since the diffraction patterns of the β phase has only four distinct peaks. This is the same conversion seen after drawing the α phase. Although the crystal structure changes with increased milling time, the peaks are less intense suggesting less crystallinity. Prolonged milling could result in a completely amorphous PVDF powder.

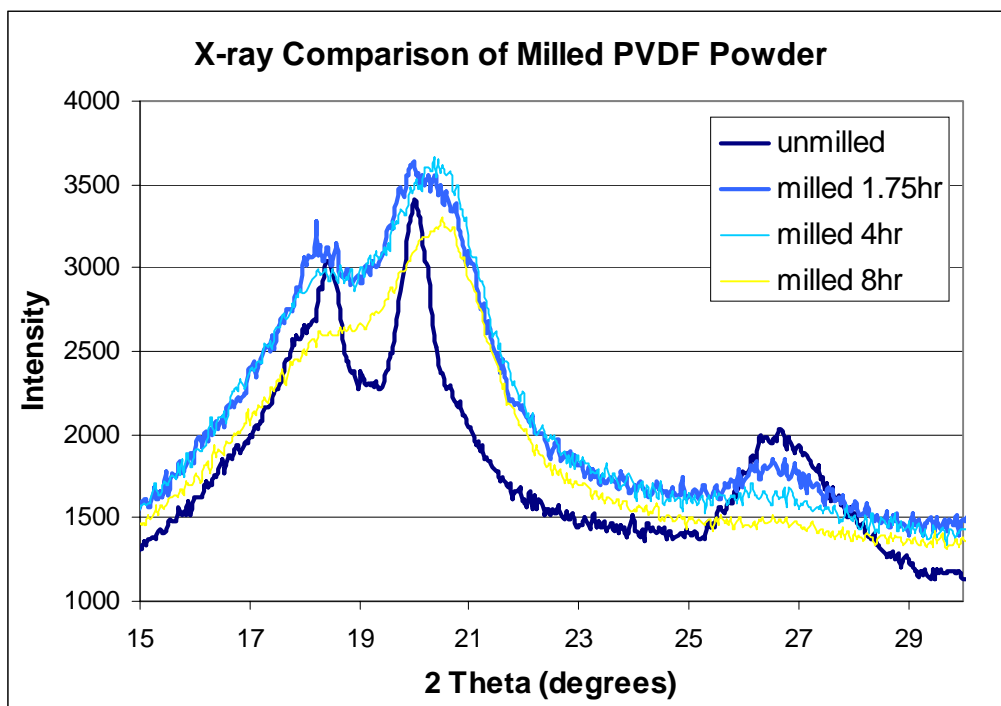


Figure 3.5 X-ray data of milled Kynar® powder. A change in the crystallinity of the Powder can be observed.

Changes in crystalline structure have been observed in similar experiments by other researchers, however no other instances were found in which PVDF was used. Castricum and coworkers⁽³⁶⁾ observed changes in the crystalline structure of polyethylene. Through milling



times of up to 165 hours they were able to change PE from an orthorhombic to a monoclinic crystal structure. Pan and Shaw⁽³⁴⁾ also observed changes in crystal structure as well a significant reduction in crystallinity. They also retained the crystal structure through a processing method using temperatures below the melting temp of the polymers and high pressures. Similarly, the diffraction peaks of the milled PVDF remained the same when the powders were sintered implying the sintered films retained the crystalline structure of the milled powders. Pressing films at high pressure and below 80° produced consistent films of uniform thickness with no change in crystallinity. Figure 3.6 shows the diffraction patterns of the sintered films and additional x-ray diffraction plots can be seen in the Appendix.

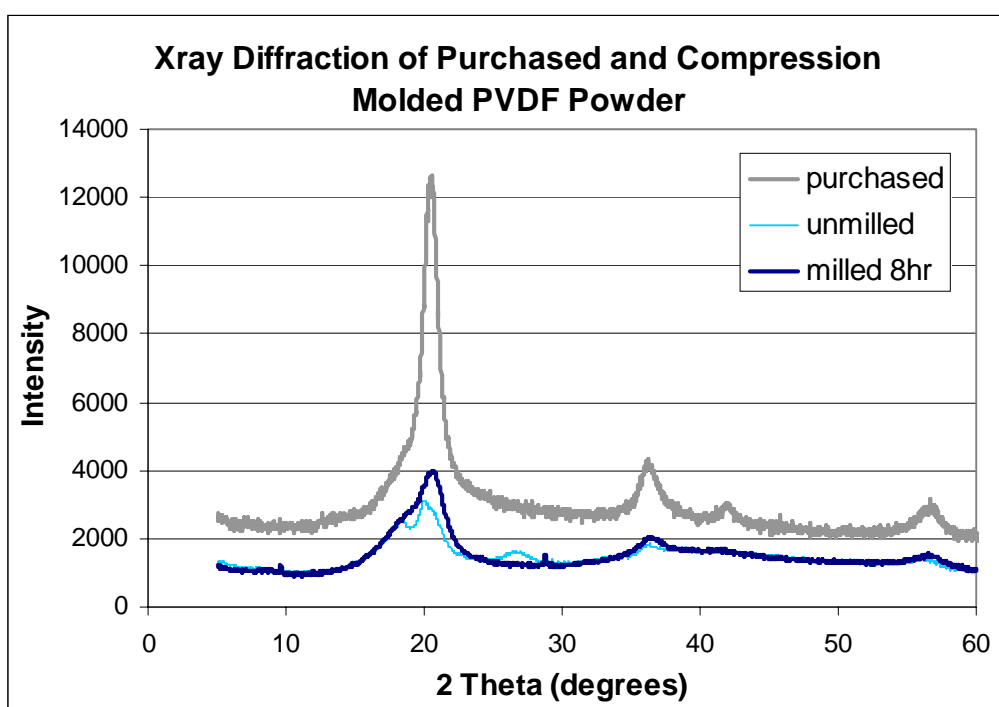
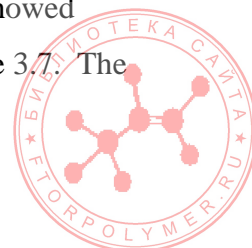


Figure 3.6 X-ray data of milled Kynar® powder. The milled Kynar® powder showed similar crystallinity as the purchased films but not the same level.

3.2.2 Scanning Electron Microscopy (SEM)

The photographs from scanning electron microscopy (SEM) of the Kynar® powder showed very uniform and spherical particles. The uniform spherical shape of the PVDF powder was expected as the raw powder had not been subjected to any mechanical processing such as grinding or cutting during its manufacturing. After milling the Kynar®, the particles showed significant deformation and fracture. The effects of milling are clearly visible in Figure 3.7. The



sharp edges and irregular shapes are a result of the repeated fracture and cold welding of the particles during milling.

While taking the SEM photographs, movement of the milled particles was observed at 8,000x magnification. However, movement was not observed with the unmilled particles. Since the samples were subjected to an electric field while in the microscope the movement could be explained by a sudden polarization or a piezoelectric response brought on by the field. PVDF in general is sensitive to strong electric fields, which can bring about changes in polarization or crystal structure. The stressed nature or presence of the β phase in the milled Kynar® could cause a response to an electric field that would not be present in the α phase of the unmilled powder⁽³⁹⁾. A strong electric field will cause a spontaneous alignment of the dipoles in β PVDF as well as a contraction along the carbon chains due to PVDF's piezoelectric properties. Also, these movements may be a result of damage to the polymer due to the strong electric fields.



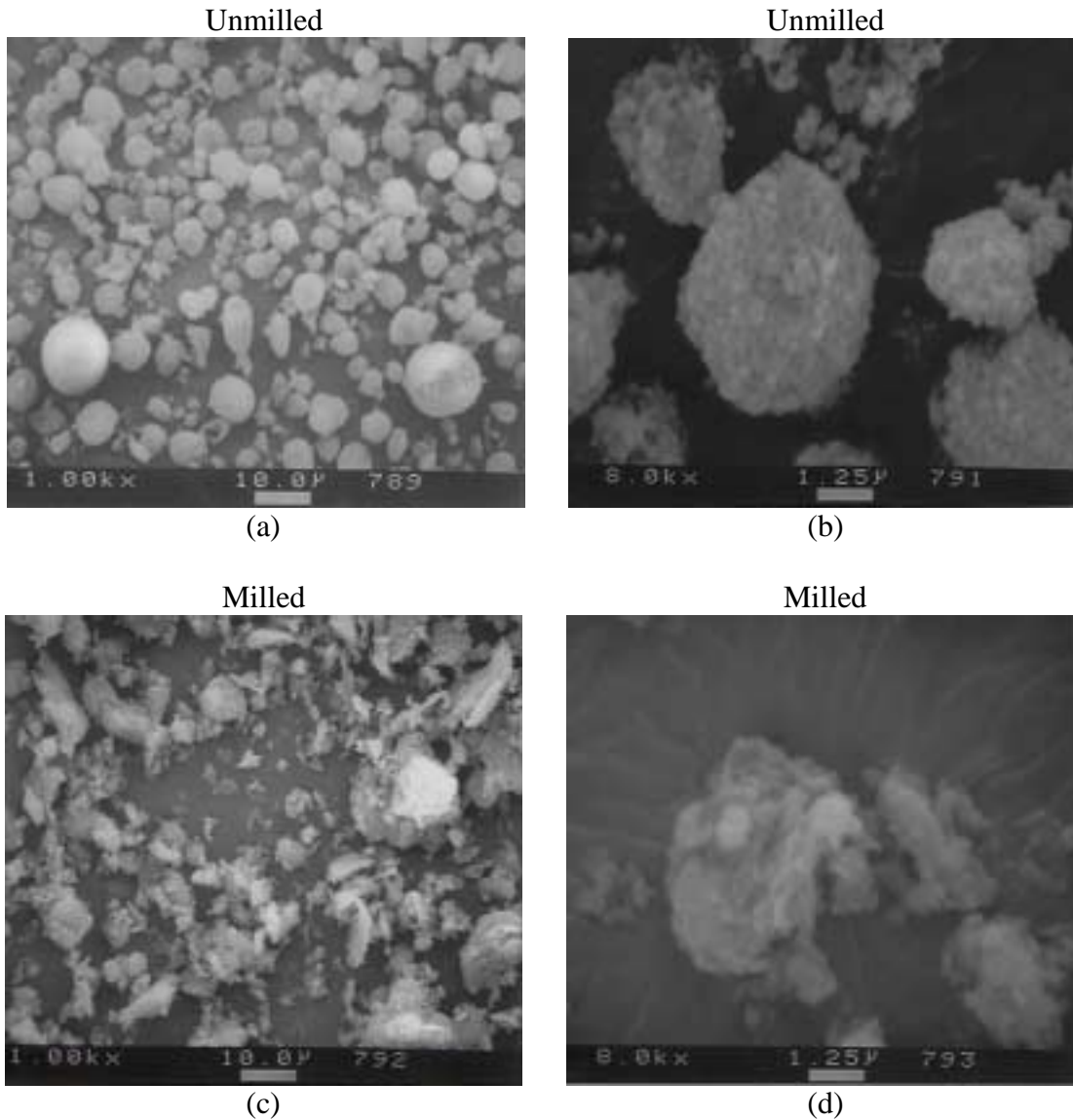
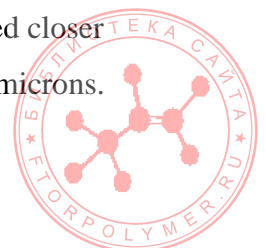


Figure 3.7 SEM Pictures of milled and unmilled Kynar® powder. (a) Unmilled 1000x magnification. (b) Unmilled 8000x magnification. (c) Milled 1000x magnification. (d) Milled 8000x magnification.

A visual comparison of the virgin and milled powders showed the average particle size of the milled powder to be only slightly smaller than the unmilled Kynar® powder. Five samples of the milled and unmilled powders were examined with each sample containing between 15 and 20 particles. The average size of the Kynar® powder observed was 4.6 microns, which is consistent with the 5.0-micron size reported by Atofina. After eight hours of milling, the average size was reduced to 3.8 microns. Also, as can be seen in Figure 3.8, the milled powder size distribution was more uniform. The particle size of the milled samples was concentrated closer to 4 microns, while the unmilled samples were distributed over a range between 4 to 6 microns.



This subtle change in particle size and distribution was to be expected due to the force of cryogenic milling. The particle size reduction and the irregular shapes of the milled particles increase the surface area of the particles making them more suitable for sintering or compression molding. Extended milling times should produce a more concentrated distribution of particles.

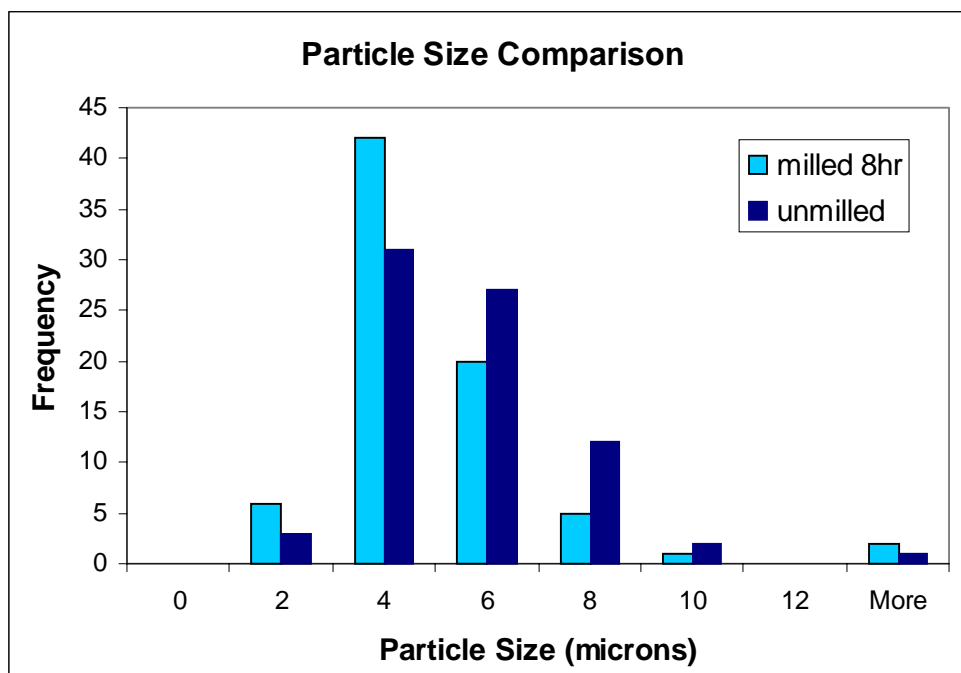


Figure 3.8 Comparison of particle sizes between milled and unmilled Kynar® powder. The processed powder had a slightly narrower distribution of particle size.

The sintered films were not of the same quality of the pressed films, they were fairly transparent but did not have the same strength and flexibility as the pressed films. Scanning electron microscopy of the sintered films showed a very smooth surface under low magnification. But, as can be seen in Figure 3.9, closer inspection at higher magnification showed the sintered films contained bumps and ridges that appeared to be remnants of the powder. Sintering of the powders was not able to produce a uniform film since some evidence of the powder still existed. The milled powders produced more uniform films than the unmilled powders. The color and strength was more consistent throughout the samples.



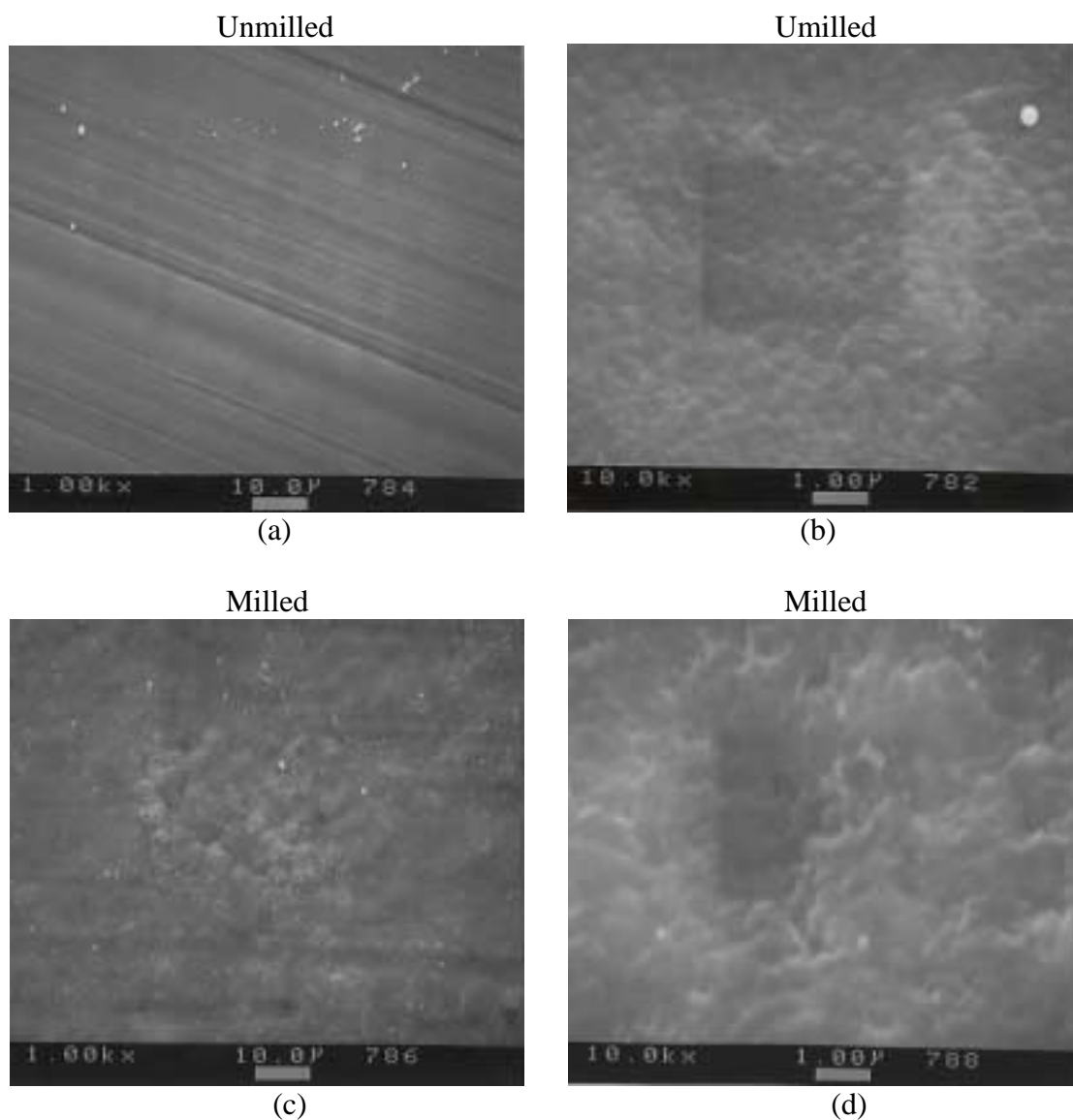


Figure 3.9 SEM pictures of sintered PVDF films. (a) Unmilled 1000x magnification. (b) Unmilled 10,000x magnification. (c) Milled 1000x magnification. (d) Milled 10,000x magnification.

3.3 In-Situ Mechanical Testing

Through the mechanical testing of materials, various material properties can be characterized, such as strength, stiffness, and toughness as well as their time and temperature dependence. By using in-situ testing techniques, poled PVDF can be measured as the sample is being subjected to an electric potential, current, or field. For materials that exhibit piezoelectric, ferroelectric, or electrostrictive properties, changes in mechanical properties can be observed as a



sample is subjected to various external electrical stimuli. For these particular experiments, it is desired to find a relationship between applied electric potential and elastic modulus.

3.3.1 In-Situ Creep Testing

For each set of experiments at a given voltage the averaged or overall change in stiffness was observed, see Figure 3.10. Although the magnitude of response was not completely reproducible, the responses to the biased voltage conditions were reproducible. Individually, the effect of biasing on the films was small, and some variations between each set of experiments at the electric potential were observed.

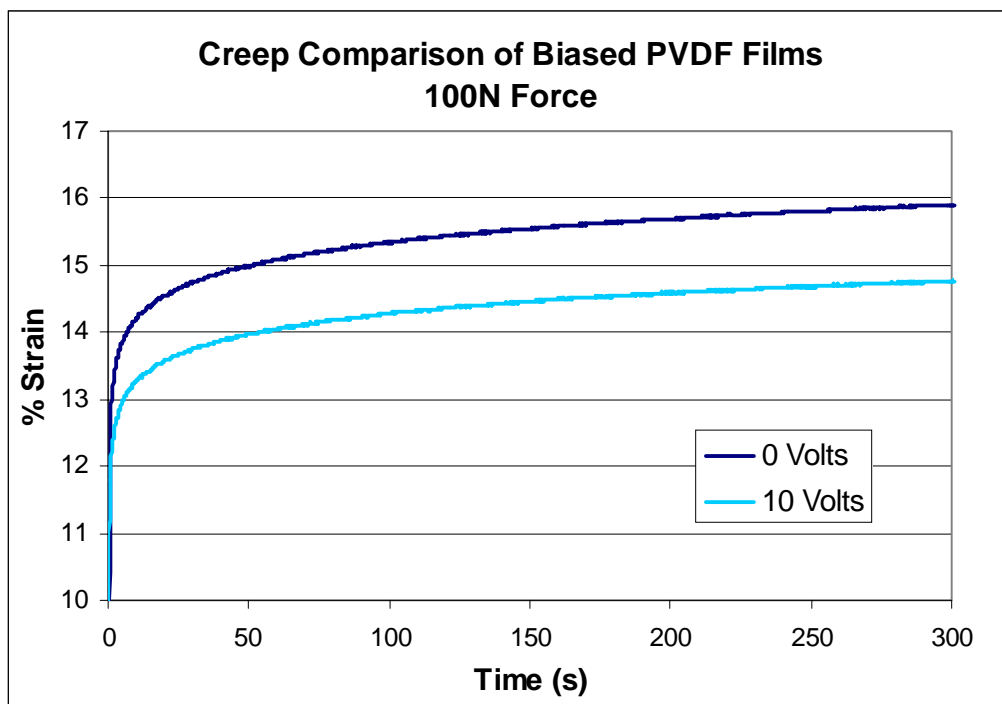


Figure 3.10 In-situ creep testing of biased PVDF film. Biased films show an increase in stiffness.

The largest change in stiffness occurred between 0 and 10 V DC, and then gradually increased up to 40 V. This response is illustrated in Figure 3.11. At 50 V, the biased conditions seemed to make the samples less stiff and more prone to creep. The decreased mechanical stiffness and increase of creep was consistent with previous experiments that show degradation of the poled structure of PVDF films. Strong electric fields and high levels of radiation can reverse the poling of piezoelectric PVDF and damage its crystal structure. Although these



experiments did not reach the 200 – 400 MV/m breakdown voltage observed in other research, the combined stress of the forces holding the samples in tension may have added to the damage observed here. Some variation occurred with each set of experiments, but the same resulting change in stiffness was consistent with each set ^(10, 24).

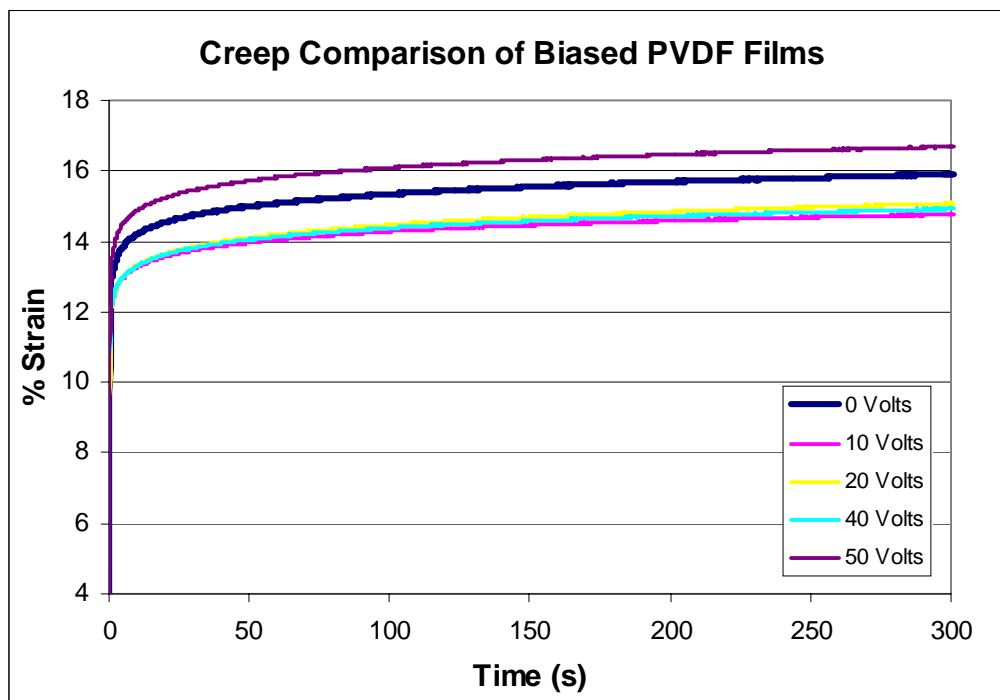


Figure 3.11 In-situ creep testing of biased PVDF film. Biased films show an increase in stiffness.

Under small loads, the degradation of the poled structure was less evident. An applied force of 50 N failed to produce a measurable change in stiffness, but the same films under a force of 100 N did produce an observable increase in stiffness. This was to be expected since an increased load would produce greater deflection and thus a more pronounced effect due to the electric field.

In order to explore the change in stiffness of the biased samples, the data was fit to a mathematical model representing the viscoelasticity of polymers (40). The four-element model was chosen because it could account for both static and dynamic responses of PVDF subjected to mechanical stress. The model takes into account the stress relaxation found during creep as well as the retarded elastic response. This model is represented by the schematic in Figure 3.12.



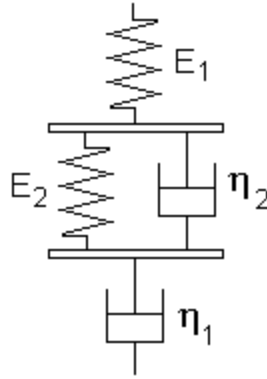


Figure 3.12 Representation of the model use to measure the creep of PVDF films.

In the model (Figure 3.12), the spring and damper in series (E_1 and η_1) represents the instantaneous and retarded elastic response respectively. The spring and damper in parallel (E_2 and η_2) represents the stress relaxation. The combination of the four elements creates the mathematical relationship given in Equation 3.1, which simulated the creep of a viscoelastic material ⁽⁴¹⁾.

$$\varepsilon = \frac{\sigma}{E_2} [1 - \exp(-t/\tau)] + \frac{\sigma}{E_1} + \frac{\sigma}{\eta_1} t \quad \text{where } \tau = \eta_2 / E_2 \quad (3.1)$$

The data for each set of experiments conducted at a particular voltage was averaged and fit to this four-element model. Figure 3.13 shows the modeled response compared to the measured values for a typical experiment. Using the model, each of the elastic and viscous parameters could be compared. The fitted parameters for each of the biased voltages are shown in Table 3.1.

Voltage	E1 (Pa)	E2 (Pa)	η_1 (s)	η_2 (s)
0	1.78E+08	2.13E+07	1.94E+10	7.28E+11
10	1.91E+08	2.25E+07	1.88E+10	7.28E+11
20	1.86E+08	2.32E+07	2.08E+10	7.26E+11
40	1.88E+08	2.27E+07	2.13E+10	7.26E+11
50	1.67E+08	2.03E+07	1.83E+10	7.26E+11

Table 3.2 Coefficients resulting from modeling the creep of PVDF films under In-situ loading.



The elastic modulus, E_1 , of PVDF is reported to be between 1000 - 3000 MPa. The values obtained were somewhat lower but proved useful for comparison purposes. One can clearly see, the values obtained from the curve fit, E_1 , show that the instantaneous elastic response changed with an applied electric voltage. The stiffness of the films increased 5.6% on average, with an applied voltage up to 40 V, and above 40 V the stiffness decreased. The decrease in stiffness may be due to PVDF's sensitivity to strong electric fields and a breakdown of the polymer's crystal structure, particularly the dipole alignment that is responsible for the piezoelectric response^(21, 22). The mechanisms responsible for the change in stiffness are undetermined from these experiments. The observed change in stiffness could be the result of a change in the elastic modulus, the piezoelectric forces of the PVDF films acting on the equipment, or more likely a combination of both.

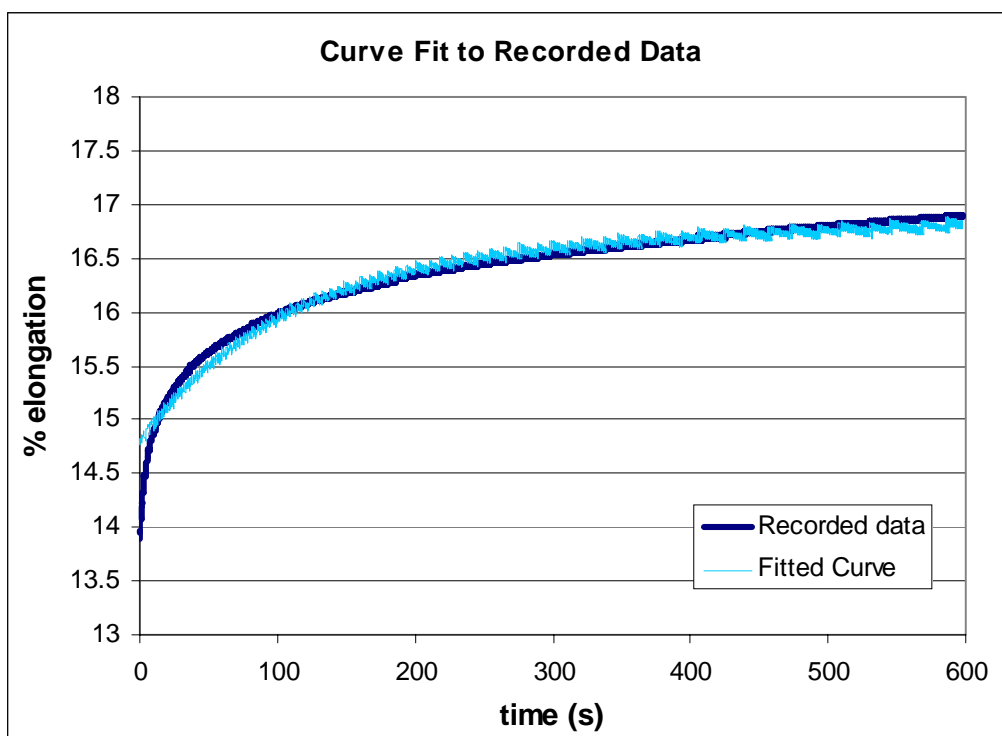


Figure 3.13 Representative curve fitting of recorded data to the four-element model.

Upon annealing, the purchased films shrunk significantly in the direction of orientation as expected for a highly oriented film. The extent of sample shrinkage increased with increasing temperature. At 130°C, the films decreased to about half their original size. Under load, the annealed films showed reduced stiffness, indicating less orientation. When biased, the films



annealed at temperatures up to 80°C exhibited a similar change in stiffness with the applied electric field. The response was significant, provided there was some residual orientation. Samples that were annealed from 80 to 130°C showed a decreasing response to the electric potential, as the orientation of the polymer chains was lost. The results of the annealed films agree with those of Wang who studied the piezoelectric effect of PVDF and its relationship to ageing and stress relaxation ⁽⁴¹⁾.

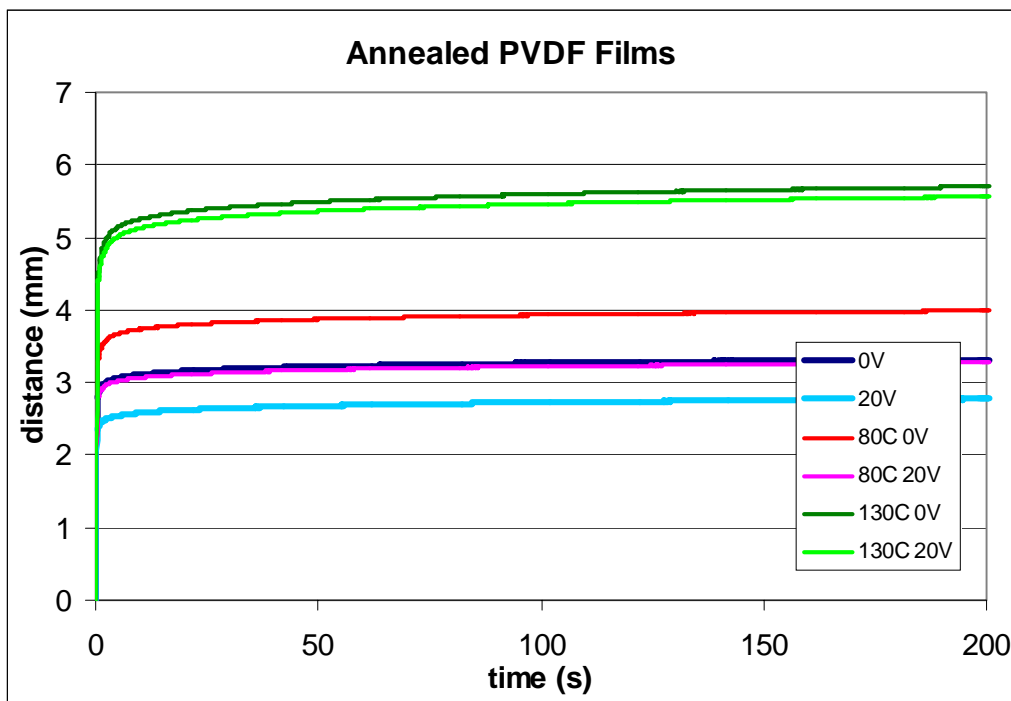


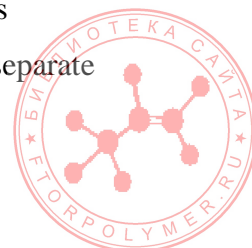
Figure 3.14 Results of the annealed films under in-situ loading.

Films pulled perpendicular to the direction of orientation deformed much more easily than those pulled in the direction of orientation. The force applied to the samples was decreased significantly to avoid failure of the sample. However, even at the decreased forces, no consistent results could be recorded for comparison. Additional plots of the in-situ creep testing can be seen in the Appendix.

3.3.2 In Situ (DMA)

3.3.2.1 Three point Bend

Measuring the change in stiffness with response to applied electric potential was successful in the creep experiments. However, more sensitive equipment is needed to separate



the change in modulus from the piezoelectric forces of the samples. By separating these two responses when biasing the samples, the extent of the change in stiffness per volt can be more closely observed. The DMA applies a user specified force to the samples and measures the storage and loss modulus with the application of that force. The equipment can make adjustments to normalize the forces being exerted by the samples piezoelectric response.

During the creep experiments on the Texture Analyzer, biasing the films with a voltage of greater than 40 V DC showed a breakdown of the piezoelectric response. Therefore, the DMA experiments limited the bias voltage to 30 V DC or less to avoid the breakdown effects from distorting the data. For comparison however, a voltage of 60 V DC was used to see if the same effect could be reproduced as in the creep experiments. The measured values for modulus are high for purchased PVDF films and this is most likely due to the silver electrodes silk-screened onto the films as seen in Table 3.2. The storage modulus changed significantly when voltage was applied with largest rate of change occurred from 0 to 10 V DC. Within the frequency range of 1 to 20 Hz there was a 14% average decrease in the storage modulus. These results are consistent with the initial elastic response of the creep experiments in which the most significant change occurred with an applied bias of 10 V DC. However, unlike the creep results, a change was measured with voltages greater than 10 V DC. There was a change of over 22% in the average storage modulus of PVDF from 0 to 30 V. The change in loss modulus was not as conclusive. The overall change in loss modulus was not as consistent as the storage modulus with increasing voltage, but on average there was a 6.9% decrease with applied voltage. The results can be seen in Tables 3.3 and 3.4 below.

Voltage (V)	Storage Modulus (MPa)	Change (MPa)	% Change
0	39500	N/A	N/A
10	34000	5500	-13.9%
20	32000	7500	-19.0%
30	30500	9000	-22.8%

Table 3.3 Changes in storage modulus observed when electrical potential is applied to PVDF films. All changes compared to 0 V.



Voltage (V)	Loss Modulus (MPa)	Change (MPa)	% Change
0	12000	N/A	N/A
10	11000	1000	-8.3%
20	11500	500	-4.2%
30	11000	1000	-8.3%

Table 3.4 Changes in loss modulus observed when electrical potential is applied to PVDF films. All changes compared to 0 V.

The storage and loss modulus are related to Young's modulus through Equation 3.2 below. The magnitude of Young's modulus, E_Y , can be found by taking the square root of the sum of the squares of the storage and loss modulus, E_S and E_L . The values for Young's modulus calculated from the DMA data are shown in Table 3.5 below.

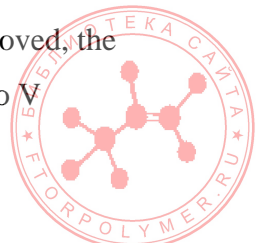
$$E_Y = E_S + iE_L \quad (3.2)$$

Voltage (V)	Young's Modulus (MPa)	Change (MPa)	% Change
0	41000	N/A	N/A
10	35500	5500	-13.4%
20	34000	7000	-17.1%
30	32500	8500	-20.7%

Table 3.5 Changes in Young's modulus with applied electric potential. All changes compared to 0 V.

These results contradict those obtained through creep testing. The Young's modulus of the biased samples decreased with increasing voltage up to 79% of the recorded value at 0 V. The results of the creep experiments distinctly showed an increase in E_1 , or resistance to deformation with applied stress. These two tests, the DMA extension and creep experiments, show opposite responses to applied voltage. This suggests that piezoelectric forces had more of an influence in the creep experiments. Since the DMA is able to normalize these forces, the only resistance measured was that of the storage and loss modulus.

Unlike the creep experiments, the observed results can be identified as changes in the materials modulus. The DMA cancelled out the material's piezoelectric forces and only changes in stiffness were measured. The results of the three point bend tests showed a change in mechanical properties with applied bias potential. However, when the voltage was removed, the storage and loss moduli did not return to their original state. The tests conducted at zero V



showed a higher storage and loss modulus than the tests with an applied biased voltage. Both storage and loss modulus decreased with increasing voltage, as shown in Figures 3.15 and 3.16, but when the voltages were removed, the modulus did not return to its original measured value.

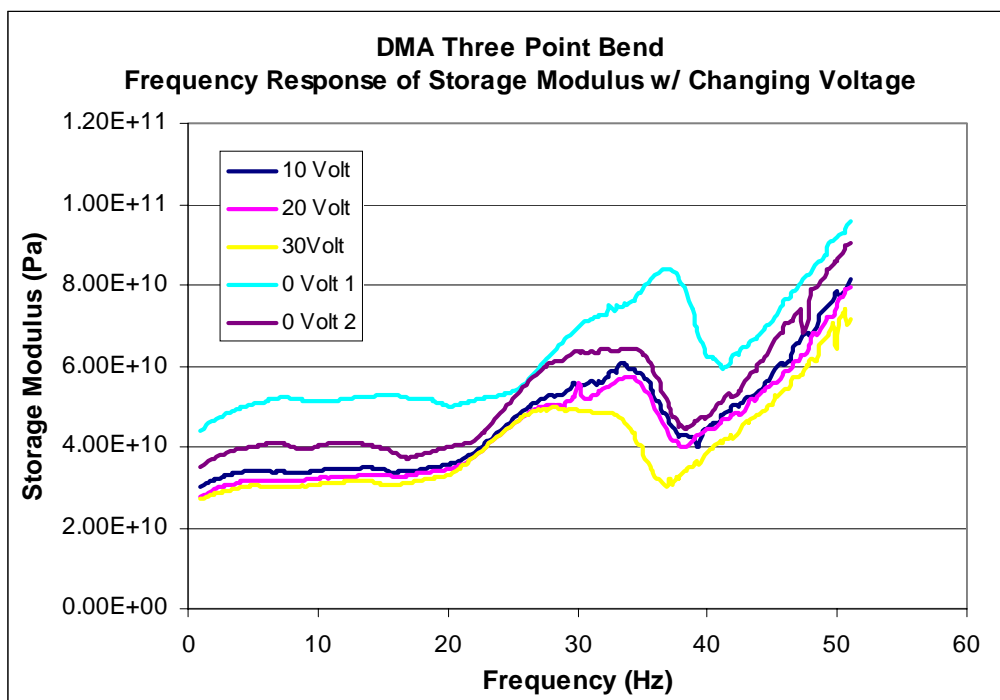


Figure 3.15 In situ biased PVDF films under DMA in three point bend. Decrease in storage modulus observed.

To ensure that no residual potential remained in the films after the potential was removed, the two electrodes were shorted to ground, to cancel any residual electrical potential. Even with the grounded electrodes the initial measurement could not be reproduced. No forces were applied that would have damaged the samples. Therefore the difference between sequential tests, without an applied potential, most likely resulted from a breakdown in the poled and aligned crystal structure due to the applied voltage. This breakdown could increase with extended durations of applied voltage but no additional change was observed in these experiments.



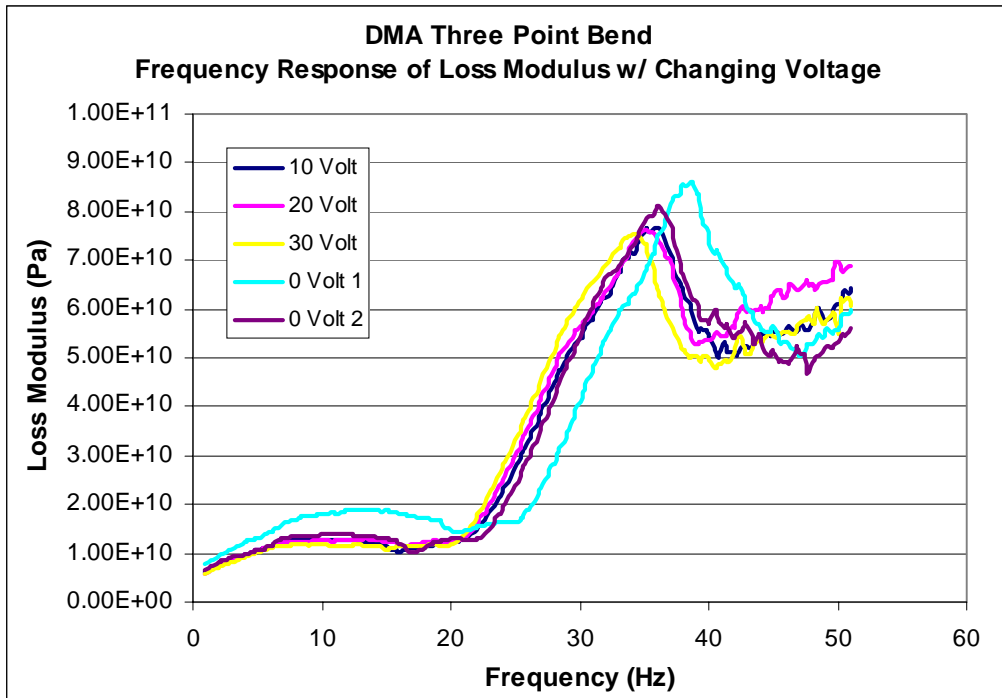
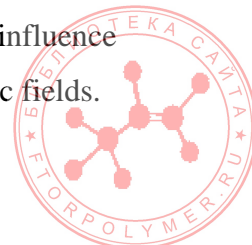


Figure 3.16 In situ biased PVDF films under DMA in three point bend. Decrease in loss modulus observed.

3.3.2.2 Extension

The extension experiments were performed using a dynamic mechanical analysis set up much like the creep experiments on the Texture Analyzer. Because the DMA is very sensitive, careful attention was paid to reducing the size of the electrodes and the effect they had on the measurements.

No change in modulus could be observed in the extension DMA experiments. Results similar to the creep experiments were expected, especially those pertaining to the degradation of the crystal structure above the critical voltage. However, no correlation between the voltage and the material's response, degradation or otherwise, was found. As can be seen in Figures 3.17 and 3.18, no net change in loss or storage modulus can be seen with applied voltage. The modulus fluctuated with different levels of electric potential, especially in the storage modulus, but no pattern arose. Smaller samples of PVDF were used for the extension experiments because of the nature of the tests. The purchased films have the same amount of silver on the surface regardless of the thickness of the films and the same amount of copper tape was used on the samples. The combination of the silver paint and the copper tape could have had a more pronounced influence on the smaller samples, causing them to show little or no response to the applied electric fields.



This stiffening of the films due to the electrodes was also experienced by Guillot et al. ⁽¹⁸⁾ who was developing ways to measure piezoelectric coefficients without electrodes. Thicker films used in the extension setup proved too stiff to produce amplitudes within the accepted bounds of the equipment.

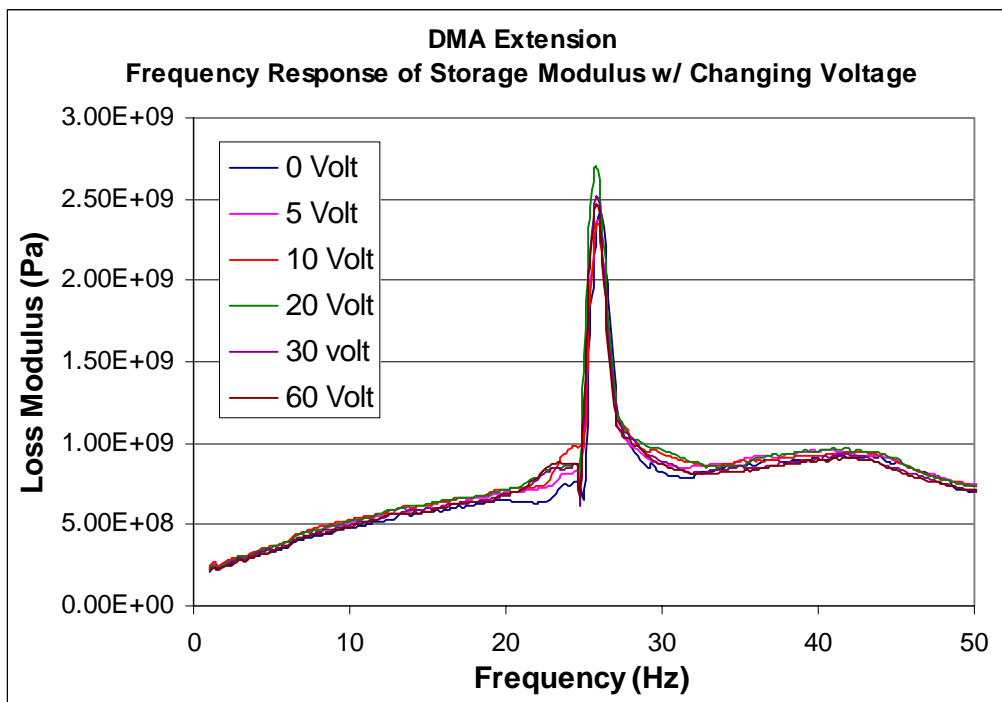


Figure 3.17 In situ biased PVDF films under DMA in extension. No changes could be observed.



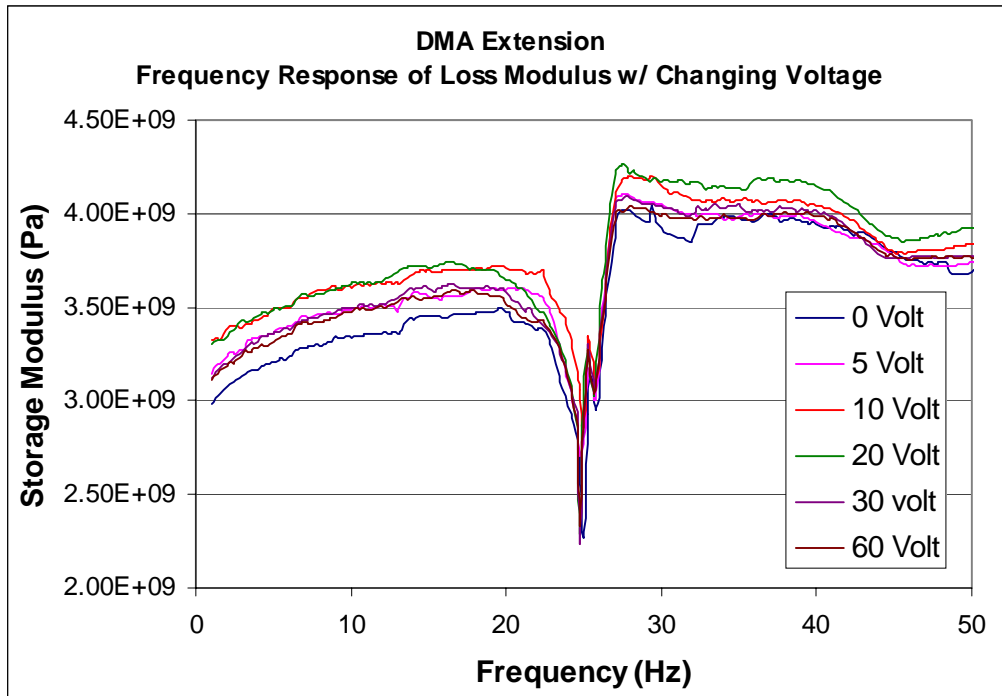


Figure 3.18 In situ biased PVDF films under DMA in extension. No changes could be observed.

A peak and/or valley were observed in all of the DMA frequency sweeps. The peaks, occurring between 20 and 40 Hz, can be seen clearly in Figures 3.15 through 3.18 and are most likely attributed to a resonant frequency of the combined PVDF film and test equipment. The data recorded from frequency scans on the equipment should appear as a flat to an increasing line with minimal bumps or peaks. At first the peaks were thought to indicate the electrodes were becoming unattached from the PVDF films, but the peaks also occurred when no electrodes were attached to the samples. With an increase in applied voltage, the location of the peaks changed suggesting a change in natural frequency of the system. This would be consistent with a change in damping coefficients in the samples. Table 3.6 shows the peak values of storage and loss modulus with increasing voltage. These results present us with the conclusion that not only did the DMA measure a change in stiffness for PVDF but also the PVDF samples changed the resonant frequency of the system. Addition results of the in-situ DMA experiments can be seen in the Appendix.



Voltage (V)	Frequency of Peak Storage Modulus (Hz)	Frequency of Peak Loss Modulus (Hz)
0	37	39
10	33	35
20	33	35
30	28	34

Table 3.6 Changes in the frequency of observed peaks during three point bend DMA testing.



Chapter 4 Conclusions

4.1 Sample Preparation

4.1.1 Hot Pressing Films

No β phase films could be formed without drawing and no films could be produced without α phase. Quenching PVDF films into liquid nitrogen from well above PVDF's melting temperature still produced crystalline samples. The differences in crystallinity between samples that were quenched and samples equilibrium cooled were minimal suggesting that crystal growth in PVDF was fast and did not rely heavily on the rate of cooling. This presented great difficulty in obtaining crystalline phases other than α which PVDF forms readily from a molten state. Annealing β phase PVDF at elevated temperatures changed the crystal structure. This confirmed the β phase's instability at high temperatures and the necessity for compression molding or sintering below 80°C to obtain piezoelectric PVDF in forms other than films.

4.1.2 Preparation of Purchased Films

Measured values of storage and loss modulus obtained from the DMA as well fitted values obtained from the creep experiments did not match accepted values of moduli for PVDF. It is believed that the silver electrodes painted on the films greatly influenced some or all of the experiments. Those tests performed in extension on the DMA would have been influenced the most since the films used for those experiments were the thinnest. The attached wires are also believed to have greatly influenced the experiments.

4.2 Material Characterization

The milling of α phase PVDF polymer showed definite indications of the formation of the β phase crystal structure. Cryogenic ball milling for extended periods of time successfully converted α phase PVDF to β . Further milling of the powders began to decrease the crystallinity of the polymer. The milled powders also showed a narrower particle size distribution, which created a more uniform film when sintered. Sintering of PVDF polymers produced brittle but uniform films that retained the crystalline structure of the milled powders plus showed signs of improved orientation. No reduction of crystallinity or change in crystal structure was observed



during compression molding. These results are important steps in finding a way to manufacture piezoelectric PVDF for a wider range of applications. A refined milling process and improved compression molding techniques for PVDF powders could prove to be an excellent way to produce complex three-dimensional shapes and increase the number of applications in which piezoelectric PVDF is used.

4.3 In-Situ Mechanical Testing

4.3.1 Creep Testing

In-situ, creep tests showed an increase in overall stiffness of the polymer films. The degree of change was significant but was not consistent between sets of experiments. Inconsistency was most likely attributed to the insensitivity of the equipment and slippage of the samples within the grips. Applied voltages greater than 40 V showed signs that the piezoelectric response of the films started to break down. This finding was consistent with other claims of a breakdown voltage for piezo-polymers in the similar voltage range and is attributed to the reversal of the poling responsible for PVDF's piezoelectric characteristics.

To study overall stiffness of the films, smaller forces were used that did not deform the samples. Smaller forces allowed the measurement of PVDF's storage and loss modulus without destroying them. The Texture Analyzer could not measure changes when the films were subjected to these smaller forces so the results were largely based on the films ability to resist deformation. Although these experiments produced valuable and interesting data they could not be used to draw the desired conclusions.

The biased creep testing of the piezoelectric films using the Texture Analyzer produced a significant increase in the measured stiffness. The magnitude of the increase could not be quantified because the results could not be consistently reproduced. Between experimental sets the change in stiffness was not constant and the only conclusion that could be drawn was that there was an increased stiffness. This observed increase in stiffness could be attributed to changes in PVDF's elastic modulus, contraction of the forces due to piezoelectric forces, or both. To quantify the stiffness changes a more sensitive apparatus like dynamic mechanical analyzer, or DMA, was used.



4.3.2 In-Situ Dynamic Mechanical Analysis

Using DMA equipment in three-point bend mode, the results contrasting those obtained in the creep testing results mentioned above. Unlike the increase in stiffness observed in the creep experiments, a decrease in storage and loss modulus, and thus a decrease in Young's modulus, was observed with an increase in applied electric potential. These contradicting results suggest that the Texture Analyzer was measuring more of the piezoelectric forces produced by PVDF and less of the changes in material properties that was desired.

While running DMA experiments, peaks in the data were observed that were attributed to the natural resonance of the system. These peaks shifted lower in frequency with increasing voltages. The shift in the peaks corresponded to a shift in the resonant frequency of the system. This would once again confirm a change in the storage and loss properties of the PVDF films. In general, more consistent and definitive results were obtained by using the DMA and overall these results were the most significant of the tests performed in this paper. A change in stiffness was confirmed due to changes in storage and loss modulus. Also the stiffness of the system can be influenced due to the piezoelectric forces of the polymer.

After the electric field was removed, the film properties did not return to their initial properties. The strong electric fields may have permanently damaged the material or the films may have required conditioning. Conditioning the polymers should be considered as part of any additional research in this area. If conditioning is required, absolute values should be made after the conditioning process achieve reproducible results. Extension on the DMA equipment did not show any change in material properties.

The presence of the metal electrodes on the surface stiffened the films and may have influenced the response of the material. Since the equipment was not designed for these types of experiments, other equipment related problems might have had influence on the results. These problems were reflected as spikes in data from the DMA and slipping of samples in the grips of the Texture Analyzer. Great care was taken to minimize these problems, but inconsistencies in the data could indicate some equipment problems still existed. Guillot and coworkers have discussed these problems in subsequent papers⁽¹⁸⁾. The results obtained from these experiments did show changes in elastic modulus. More sensitive equipment, designed for in-situ testing on electrically biased films, may be able to provide more quantitative results.



4.4 Recommendations for Future Work

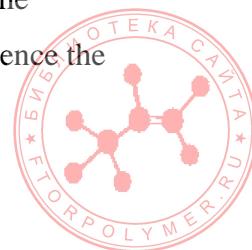
Using a dielectric analyzer, such as the TA Instruments DEA 2970 or a HP 4275A Multi-Frequency LCR Meter, may prove helpful to measure the response of the storage and loss modulus to the applied electric field. Since the electric field is already present, only the voltage potential needs to be varied to measure changes in material properties. Using a dielectric analyzer would allow measurements to be made without the presence of metal electrodes attached directly to the films. The absence of the electrodes may produce results that are more representative of the test materials response. This idea was investigated briefly, but no instrument was found where the voltage could be adjusted, and it was highly discouraged by the manufacturers to tamper with the equipment.

Additional studies to investigate crystalline structure while poled PVDF are biased could provide insight into the crystal structure rearrangements. If the PVDF films could be biased while in the x-ray diffractometer, it would be possible to measure a change in d-spacing of the crystal structure as bias potential is applied.

Ball milling PVDF powders shows many possibilities and PVDF has shown to hold its crystal structure when sintered. If a process were developed, where PVDF shapes could be produced below 80°C, it is possible that piezoelectric devices could be made in any size and shape. Currently piezoelectric PVDF devices are limited to those manufactured from films. The use of films greatly limits PVDF applications, areas such as actuators and dampers. It may be possible to expand the range of uses for piezoelectric PVDF if β phase powders could be sintered into custom shapes. If electrostrictivity of un-oriented PVDF are proves useful, sintering of β phase powders could warrant further investigation.

There are many PVDF copolymers that exhibit piezoelectric behavior. The properties of existing copolymers might be enhanced and new copolymers identified through mechanical alloying powdered PVDF copolymers. The same experiments performed in this paper could be used, with the many PVDF co-polymers, combinations of PVDF co-polymers, or a combination of PVDF polymers and piezoelectric or ferroelectric ceramics.

Optimizing the milling process for the PVDF polymers and co-polymers could be used to maximize the conversion of α phase to β , or to customize the piezoelectric abilities of the polymers. Milling times, temperatures, size and number of milling spheres, could influence the



change of the polymers crystal structure. An ideal process would use all the process variables to custom manufacture the polymer with the desired piezoelectric properties, then form the power into the desired three-dimensional shape by sintering or other process.

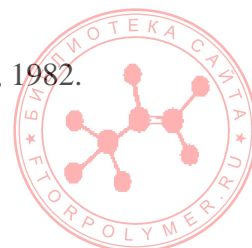


Bibliography

- 1 Rao S S, Sunar M. “Piezoelectricity and Its Use in Disturbance Sensing and Control of Flexible Structures: A survey”, Applied Mechanics Review, 47, No 4, 113-123, 1994.
- 2 Sundar V, Newnham R E. “Electrostriction”, ENGnetBASE 2000, CRC Press LLC, chap. 50, <http://www.engnetbase.com>, 1999.
- 3 Wirsen A. Electroactive Polymer Materials, Technomic Publishing, Lancaster, PA, 1986.
- 4 Bune A V, Zhu C, Ducharme S, Blinov L M, Fridkin V M, Palto S P, Petukhova N G, Yudin S G. “Piezoelectric and Pyroelectric Properties of Ferroelectric Langmuir-Blodgett Polymer Films”, Journal of Applied Physics, 85, No 11, 7869-7873, 1999.
- 5 Marutake M. “The Days When Piezoelectric PVDF Was Discovered”, Ferroelectrics, 171, 5-6, 1995.
- 6 Bar-Cohen Y, Xue T, Lih S. “Polymer Piezoelectric Transducers for Ultrasonic NDE”, NDTnet, 1, No 9, <http://www.ndt.net/article/yosi/yosi.htm>, 1996.
- 7 Furukawa T. “Ferroelectric Properties of Vinylidene Fluoride Copolymers”, Phase Transitions, 18, 143-211, 1989.
- 8 Schmidt H, Conant J, Bohannan G, Eckberg J, Halko S, Hallenberg J, Nelson C, Peterson N, Smith C, Thrasher C, Tikalsky B. “Piezoelectric Polymer Actuators for Vibration Suppression”, SPIE, 3669, 62-170. 1999.
- 9 Bohannan G W. “Piezoelectric polymer actuators in a vibration isolation application”, Smart Structures and Materials 2000, 3897, 331-332, 2000.
- 10 Lovinger A J. “Poly(vinylidene fluoride)”, Developments in Crystalline Polymers, Applied Science Publishers Ltd, Englewood, NJ, 1982.
- 11 Vinogradov A, Holloway F. “Electro-Mechanical Properties of the Piezoelectric Polymer PVDF”, Ferroelectrics, 226, 169-181, 1999.
- 12 Linares A, Acosta J L. “Pyro-piezoelectrics Polymers Materials-I. Effect of Addition of PVA and/or PMMA on the Overall Crystallization Kinetics of PVDF from Isothermal and Non-isothermal Data”, European Polymer Journal, 31, No 7, 615-619, 1995.
- 13 Destruel P, Rojas F S, Tougne D, Hoang-The-Giam. “Pressure and Temperature Dependence of the Electromechanical Properties of Polarized Polyvinylidene Fluoride Films”, Journal of Applied Physics, 56, No 11, 3298-3303, 1984.



- 14 Bar-Cohen Y, Xue T, Shahinpoor M, Simpson J O, Smith J. "*Flexible, low-mass robotic arm actuated by electroactive polymers (EAP)*", Proceedings of the SPIE International Smart Materials and Structures Conference, No 3329-07, 1998.
- 15 Vinogradov A M, Holloway F. "*Dynamic Mechanical Testing of the Creep and Relaxation Properties of Polyvinylidene Fluoride*", Polymer Testing, 19, 131-142, 2000.
- 16 Crawley E F. "*Intelligent Structures for Aerospace: A technology Overview and Assessment*", AIAA Journal, 32, No. 8, 1689-1699, 1994.
- 17 Date M, Kutani M, Sakai S. "*Electrically Controlled Elasticity Utilizing Piezoelectric Coupling*", Journal of Applied Physics, 87, No 2, 863-868, 2000.
- 18 Guillot F M, Jarzynski J. "*A New Method for the Absolute Measurement of Piezoelectric Coefficients on Thin Polymer Films*", Journal Acoustic Society of America, 108, 600-607, 2000.
- 19 Gregorio R J R, Ueno E M. "*Effect of Crystalline Phase, Orientation and Temperature on the Dielectric Properties of PVDF*", Journal of Material Science, 34, 4489-4500, 1999.
- 20 Xu H, Shanthi H, Bharti V, Zhang Q M. "*Structural, Conformational, and Polarization Changes of Poly(vinylidene fluoride-trifluoroethylene) Copolymer Induced by High Energy Electron Irradiation*", Macromolecules, 33, 4125-4131, 2000.
- 21 Scheinbeim J I. "*Poly(vinylidene fluoride)*", Polymer Data Handbook, Oxford University Press, Inc., USA, 949-955, 1999.
- 22 Inderherbergh J. "*Polyvinylidene Fluoride (PVDF) Appearance, General Properties and Processing*", Ferroelectrics, 115, 295-302, 1991.
- 23 Yang X, Kong X, Tan S, Li G, Ling W, Zhou E. "*Spatially-confined Crystallization of Poly(vinylidene Fluoride)*", Polymer International, 49, 1525-1528, 2000.
- 24 Tadokoro H. Structures of Crystalline Polymers. New York : Wiley, 1979.
- 25 Chiang L Y, Chaikin P M. "*Advanced Organic Solid State Materials*", Materials Research Society, Boston, 1990.
- 26 Hopfinger A J. Conformational Properties of Macromolecules, Academic Press, New York, 1973.
- 27 Wise D, ed. Electrical and Optical Polymer Systems, Marcel Dekker Inc., New York, 1998.
- 28 Seanor D A, ed. Electrical Properties of Polymers, Academic Press, New York, 1982.



- 29 Riande E, Siaz E. Dipole Moments and Birefringence of polymers, Prentice Hall, Englewood Cliffs, N.J, 1992.
- 30 Gregorio, R J R, Cestari M. “*Effect of Crystallization Temperature on the Crystalline Phase Content and Morphology of Poly(vinylidene Fluoride)*”, Journal of Polymer Science: Part B: Polymer Physics, 32, 859-870, 1994.
- 31 Lovinger A J, Keith H D. “*Chain Tilt in α -Poly(vinylidene fluoride)*”, Macromolecules, 29, 8541-8542, 1996.
- 32 El Mohajir B, Heymens N. “*Changes in Structural and Mechanical Behavior of PVDF with Processing and Thermomechanical Treatments*”, Polymer, 42, 5661-5667, 2001.
- 33 Smith A P, Spontak R J, Ade H, Smith S D, Koch C C. “*High-Energy Cryogenic Blending and Compatibilizing of Immiscible Polymers*”, Advanced Materials, 11, No. 15, 1277-1281, 1999.
- 34 Pan J, Shaw W J D. “*Properties of a Mechanically Processed Polymeric Material*”, Advanced Materials: Meeting the Economic Challenge, 762-775, (1992).
- 35 Font J, Muntasell J, Cesari E. “*Amorphization of Organic Compounds by Ball Milling*”, Materials Research Bulletin 32, 1691-1696 1997.
- 36 Castricum H L, Yang H, Bakker H, Van Deursen J H. “*A study of Milling of Pure Polymers and a Structural Transformation of Polyethylene*”, Synthesis and Properties of Mechanically Alloyed and Nanocrystalline Materials, 211-216, 1996.
- 37 Benjamin J S, Volin T E. “*The Mechanism of Mechanical Alloying*”, Metallurgical Transactions, 5, 1929-1934, 1974.
- 38 Hartmann B, Lee G F. “*Tensile Yield in Poly(Chlorotrifluoroethylene) and Poly(Vinylidene Fluoride)*”, Polymer Engineering and Science, 31, No 4, 231-238, 1991.
- 39 Bharti V, Shanthi G, Xu H, Zhang Q M. “*Effects of sample processing and high energy electron irradiation conditions of the structural and transitional properties of P(vdf-trfe) copolymer films*”, Electroactive Polymers, 600, 47-52, 1999.
- 40 Sperling L H. Introduction to Physical Polymer Science, John Wiley & Sons, Inc., New York, 1992.
- 41 Wang T T. “*Stress Relaxation and Its Influence on Piezoelectric Retention Characteristics of Uniaxially Stretched Poly(vinylidene fluoride)*”, Journal of Applied Physics, 53, No 3, 1828-1829, 1982.



Appendix

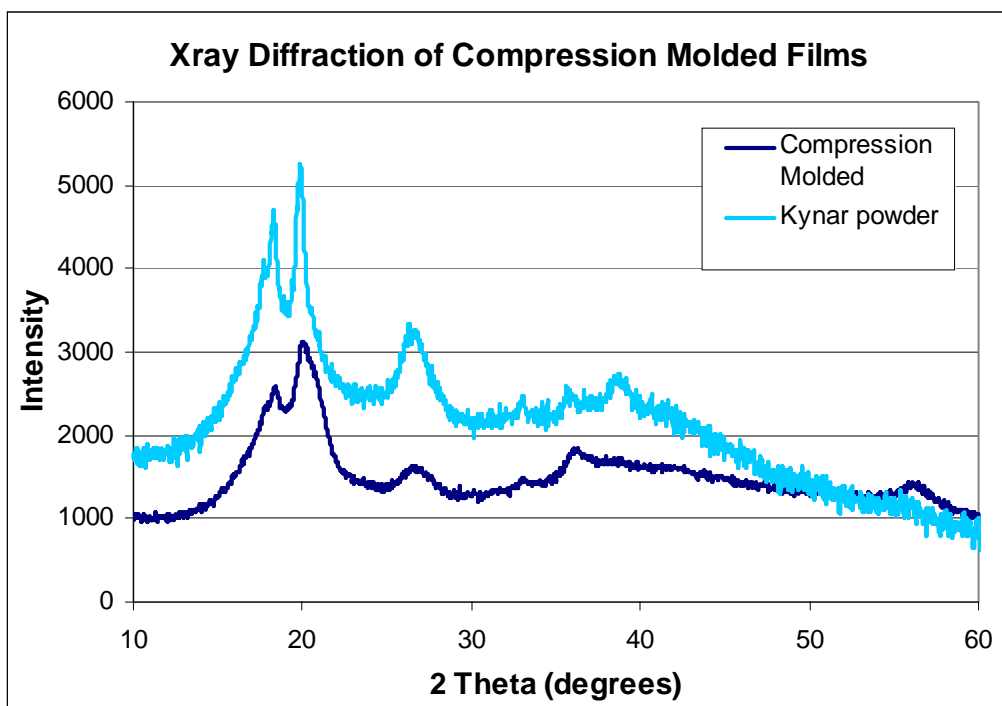


Figure A.1 X-Ray diffraction of unmilled, compression molded PVDF powder. A small decrease in crystallinity can be observed.

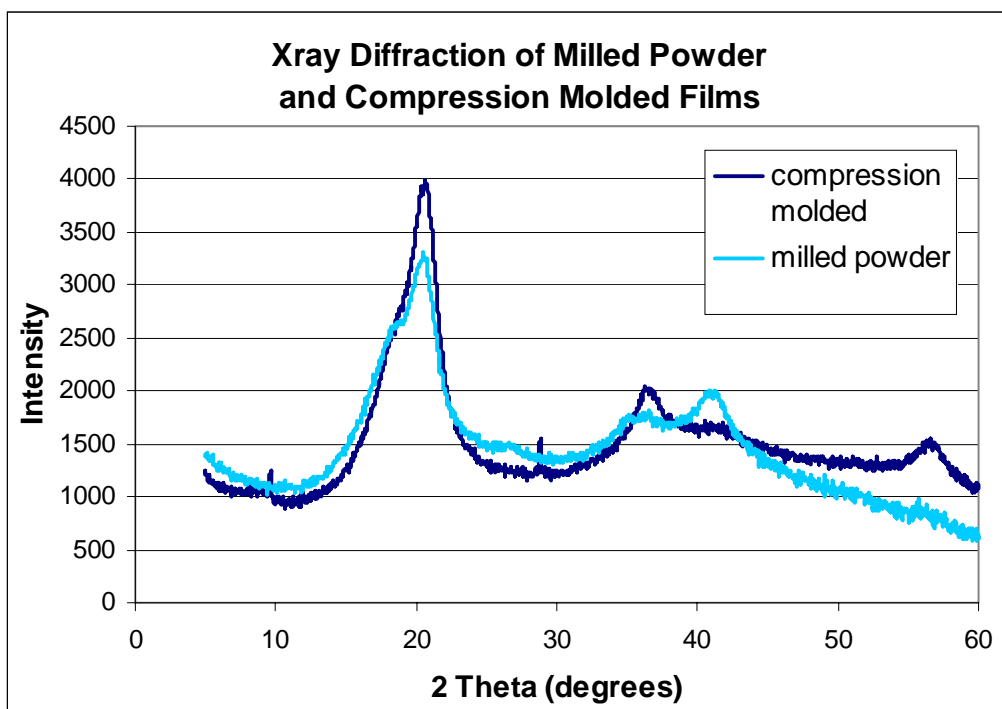


Figure A.2 X-Ray diffraction of milled, compression molded PVDF powder. A small increase in orientation may have occurred as a result of the high pressure.



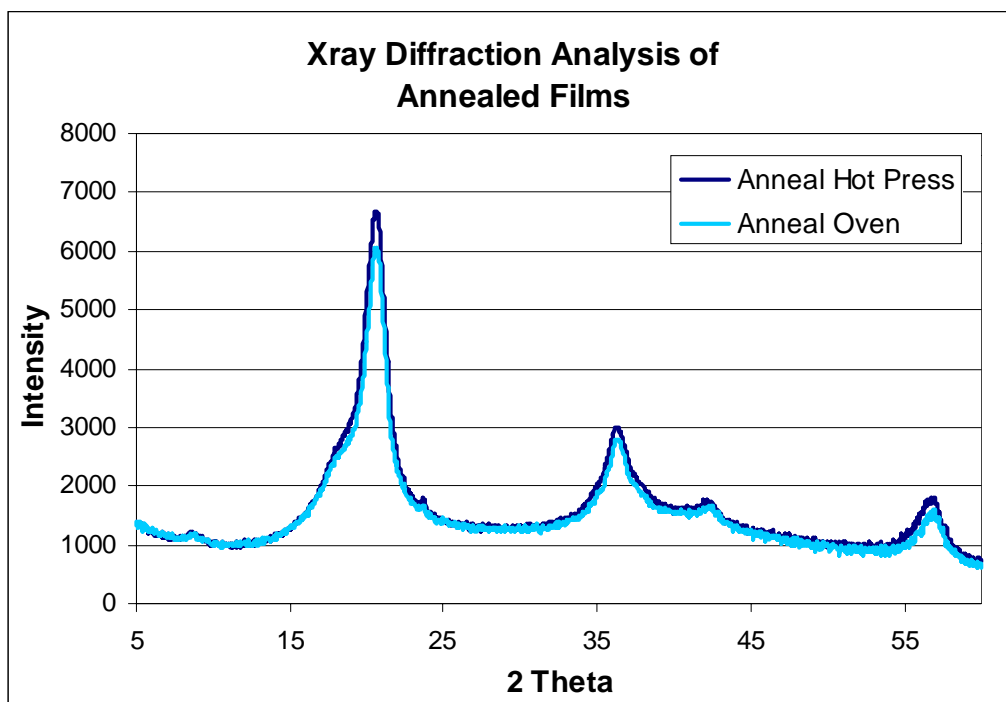


Figure A.3 X-Ray diffraction of PVDF films annealed in an oven and hot press. There is very little difference in results between the two annealing methods.

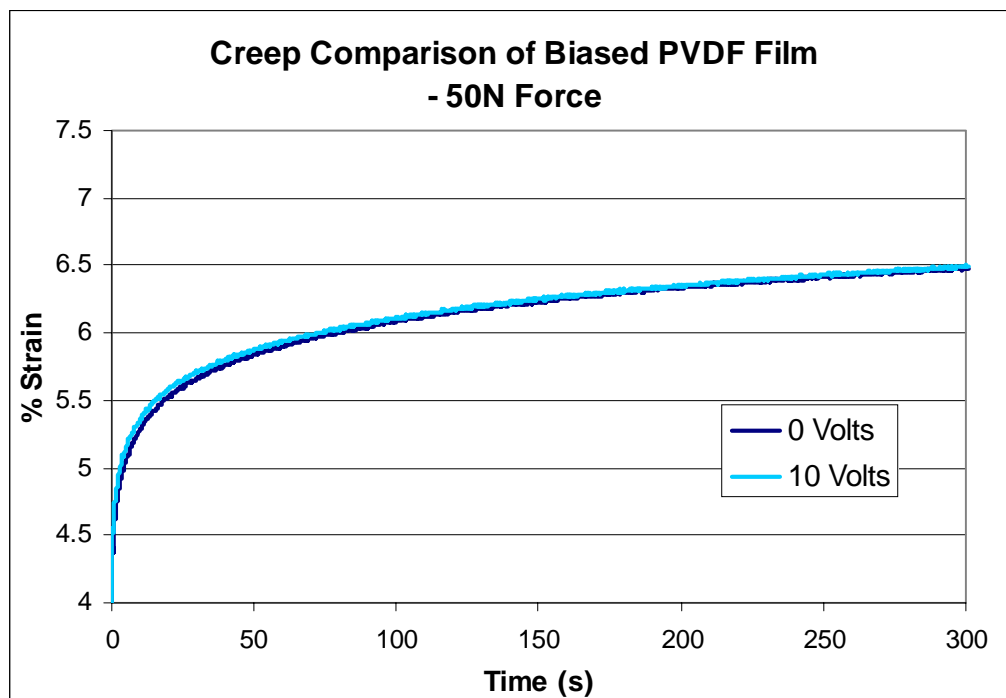


Figure A.4 In-Situ creep test of biased PVDF film. A 50 N force was applied to the samples. No change could be measured.



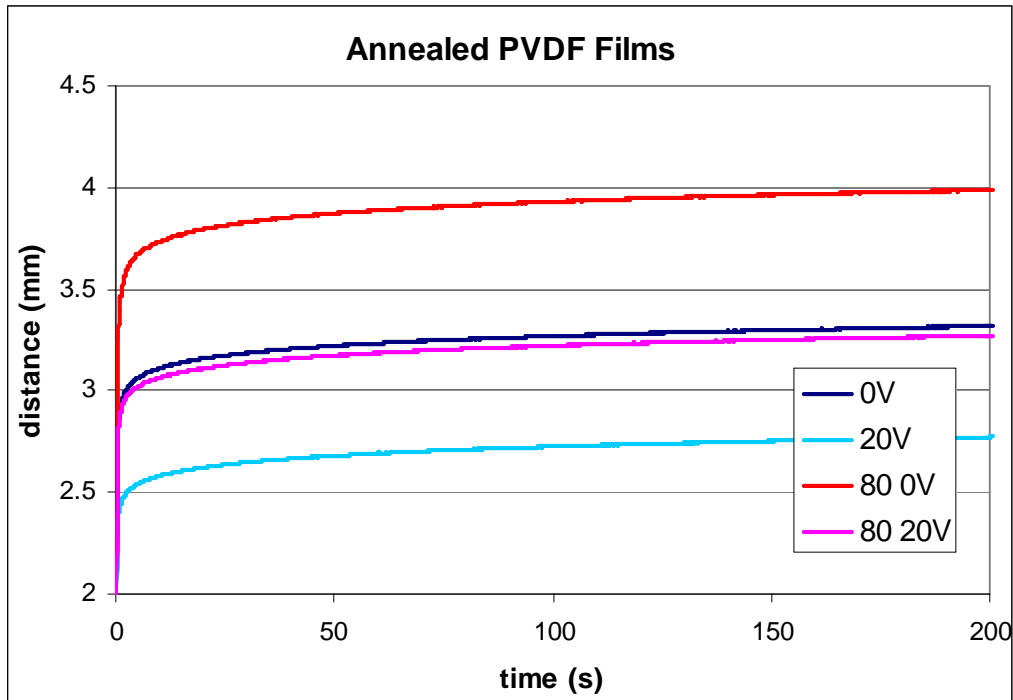


Figure A.5 In-Situ creep test of biased, annealed PVDF film. The annealed films have a lower initial stiffness but still retain the response due to the electric field.

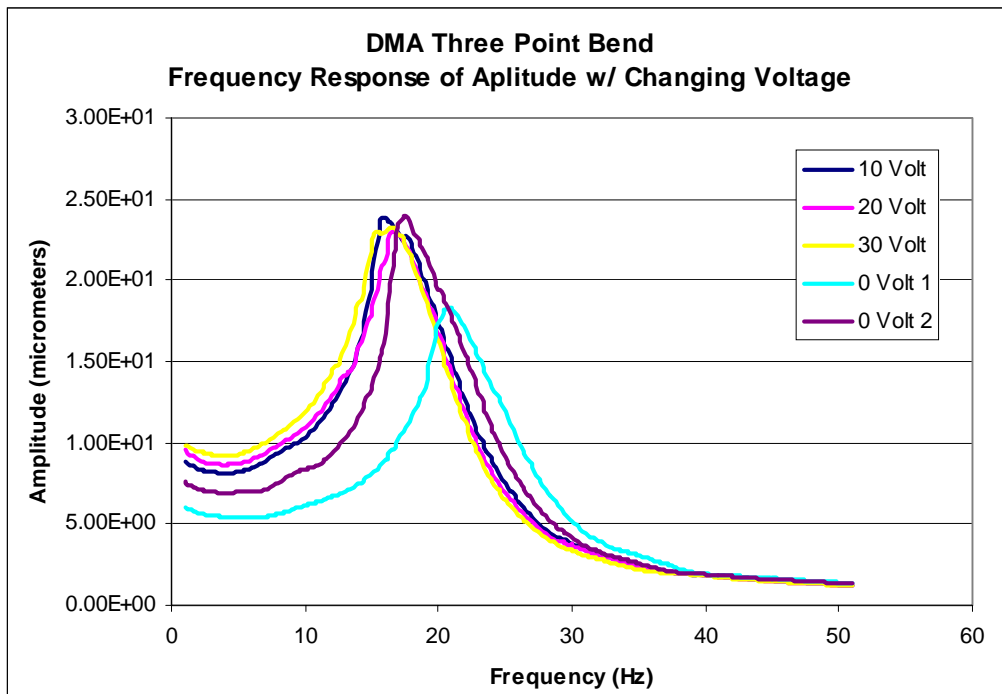


Figure A.6 DMA of biased PVDF in three point bend. An initial response occurred but the mechanical properties did not return to their original state.



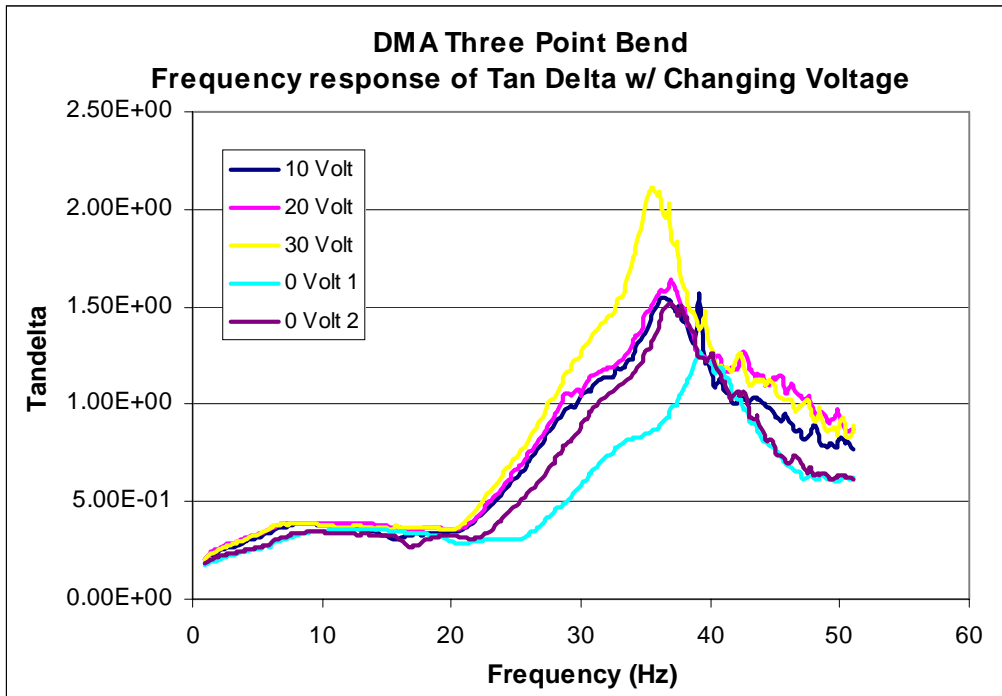


Figure A.7 DMA of biased PVDF in three point bend. An initial response occurred but the mechanical properties did not return to their original state.

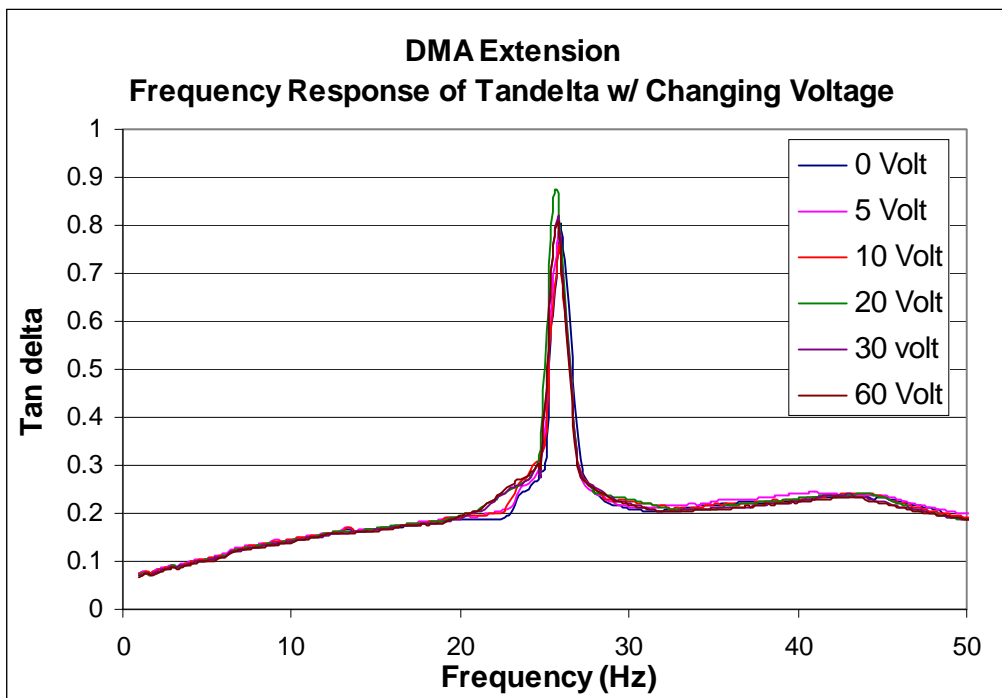


Figure A.8 DMA of biased PVDF in extension. No change in mechanical properties could be observed.



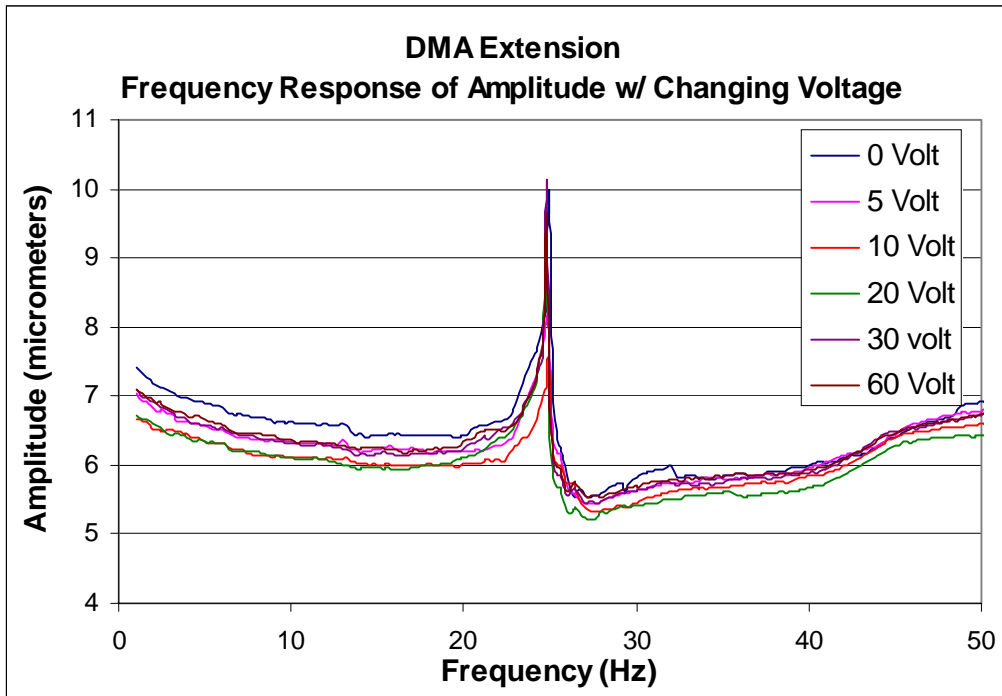


Figure A.9 DMA of biased PVDF in extension. No change in mechanical properties could be observed.

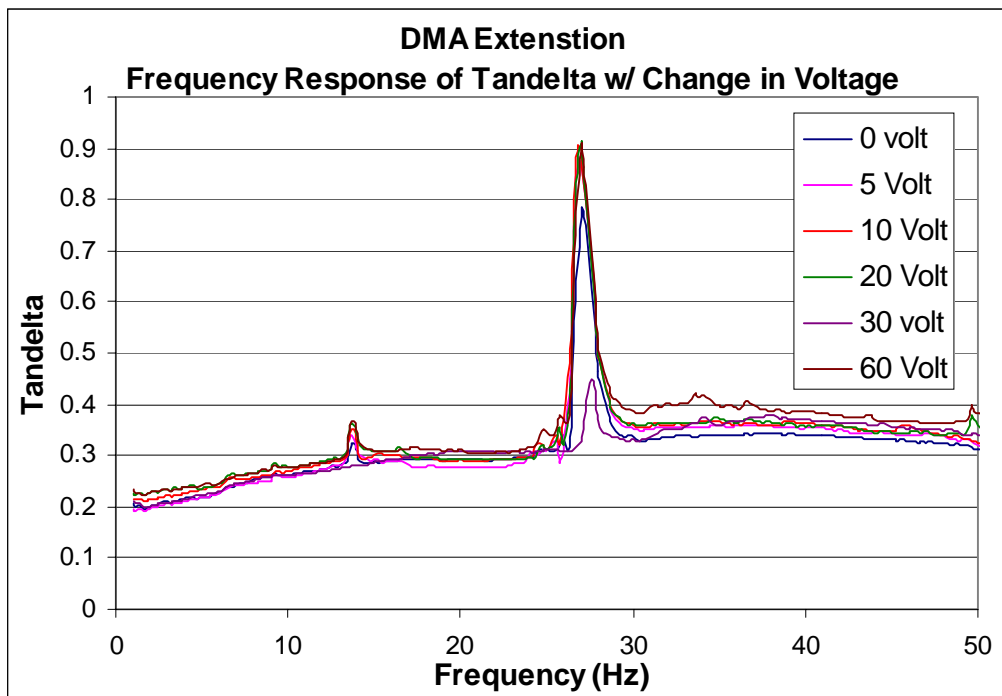


Figure A.10 DMA of biased PVDF in extension. No change in mechanical properties could be observed.



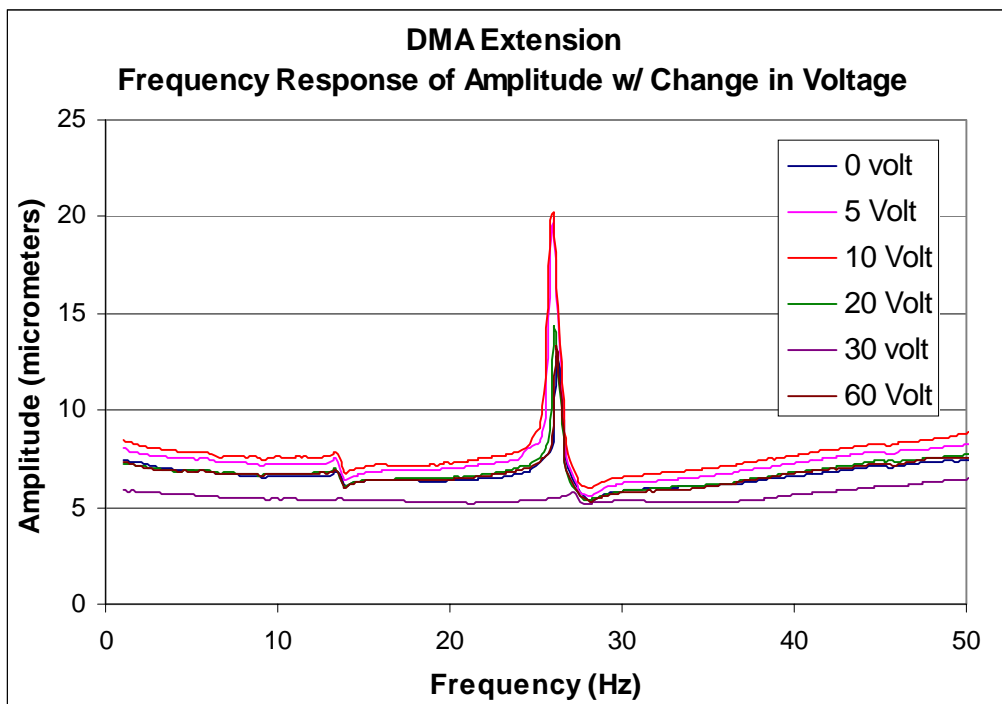


Figure A.11 DMA of biased PVDF in extension. No change in mechanical properties could be observed.

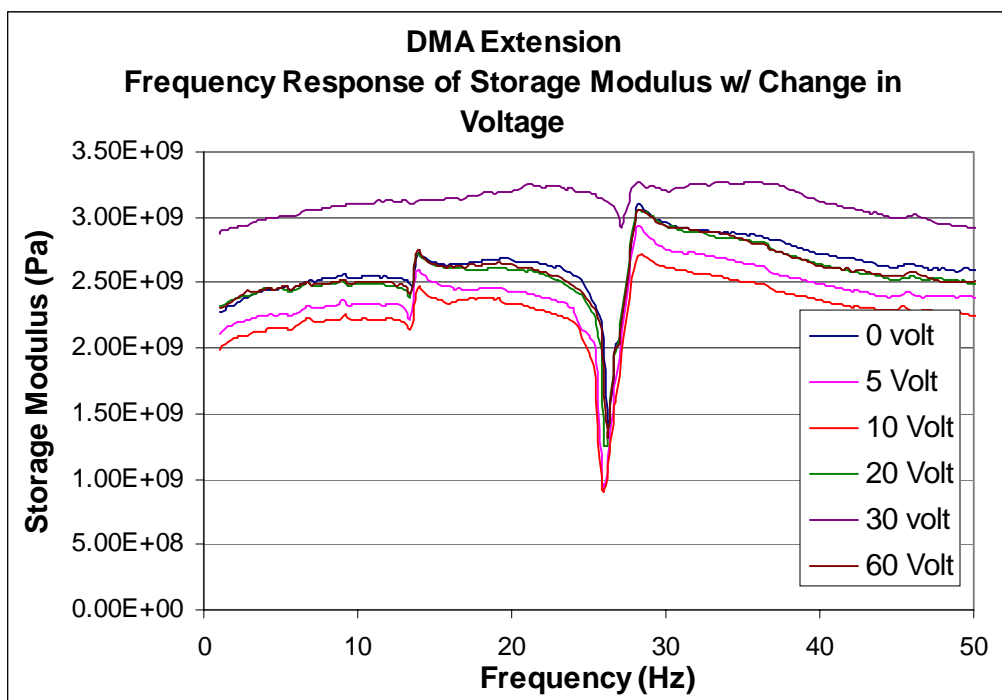


Figure A.12 DMA of biased PVDF in extension. No change in mechanical properties could be observed.



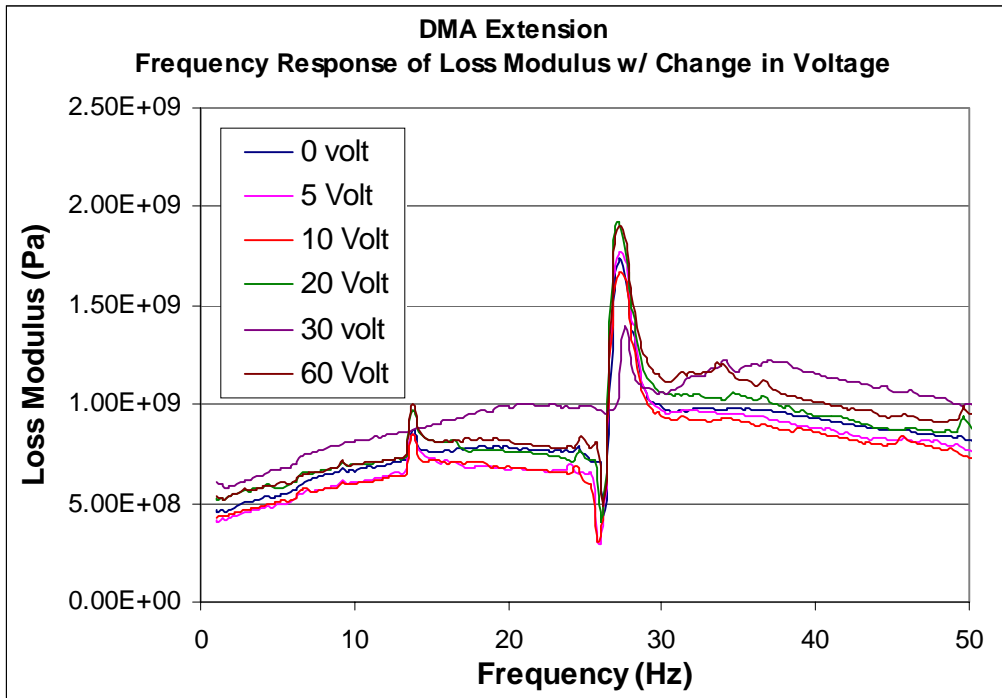


Figure A.13 DMA of biased PVDF in extension. No change in mechanical properties could be observed.

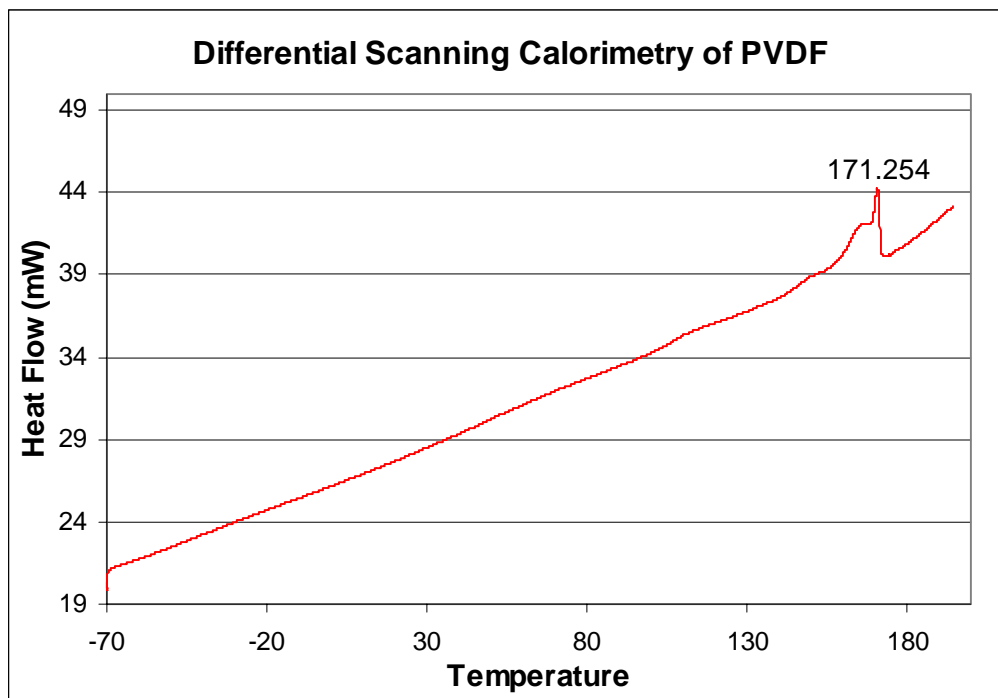


Figure A.14 DSC of Poly(vinylidene fluoride). The melting point is shown at 171°C



Vita

Daniel M. Esterly

Born in Wilmington, Delaware in 1976. Received a Bachelor's of Science degree in Mechanical Engineering from Virginia Polytechnic Institute and State University in 1999. Currently employed by Visteon Automotive Company as Design Engineer.

